# Методы и средства Цифровой Обработки Сигналов

## Свойства преобразований

Круглов Евгений Владимирович, аспирант МИФИ
Решетов Владимир Николаевич, к.ф.-м. н. доцент МИФИ.

Москва 2008

# Преобразование Фурье

$$x(n) = \frac{1}{N}\sum_{k=0}^{N-1} X(k) e^{\frac{2\pi jkn}{N}}.$$

$$X(k) = \sum_{n=0}^{N-1} x(n) e^{\frac{-2\pi jkn}{N}}.$$

$$x(n) = \frac{1}{N}\sum_{k=0}^{N-1} X(k)\exp\left(\frac{2\pi jnk}{N}\right).$$

$$X(k) = \sum_{n=0}^{N-1} x(n)\exp\left(\frac{-2\pi jnk}{N}\right),$$

$$x(t) = \frac{1}{\pi}\int_{0}^{+\infty} Re\,X(\omega)\cos(\omega t) - Im\,X(\omega)\sin(\omega t)\,d\omega$$

$$x[i] = \sum_{k=0}^{N/2} Re\bar{X}[k]\cos(2\pi ki/N) + \sum_{k=0}^{N/2} Im\bar{X}[k]\sin(2\pi ki/N)$$

$$ReX[k] = \sum_{i=0}^{N-1} x[i]\cos(2\pi ki/N)$$

$$ReX(\omega) = \int_{-\infty}^{+\infty} x(t)\cos(\omega t)\,dt$$

$$ImX[k] = -\sum_{i=0}^{N-1} x[i]\sin(2\pi ki/N)$$

$$ImX(\omega) = -\int_{-\infty}^{+\infty} x(t)\sin(\omega t)\,dt$$

$$X(k) = \frac{1}{N}\sum_{n=0}^{N-1} x(n)e^{-j2\pi nk/N} = \frac{1}{N}\sum_{n=0}^{N-1} x(n)\left[\cos(2\pi nk/N) - j\sin(2\pi nk/N)\right]$$

$$x(n) = \sum_{k=0}^{N-1} X(k)e^{j2\pi nk/N} = \sum_{k=0}^{N-1} X(k)\left[\cos(2\pi nk/N) + j\sin(2\pi nk/N)\right]$$

# Фурье

EQUATION 10-1
The DTFT analysis equation. In this relation, $x[n]$ is the time domain signal with $n$ running from 0 to $N-1$. The frequency spectrum is held in: $Re X(\omega)$ and $Im X(\omega)$, with $\omega$ taking on values

$$Re X(\omega) = \sum_{n=-\infty}^{+\infty} x[n] \cos(\omega n)$$

$$Im X(\omega) = - \sum_{n=-\infty}^{+\infty} x[n] \sin(\omega n)$$

$$Re \bar{X}[k] = \frac{Re X[k]}{N/2}$$

$$Im \bar{X}[k] = - \frac{Im X[k]}{N/2}$$

$$x[n] = \frac{1}{\pi} \int_0^{\pi} Re X(\omega) \cos(\omega n) - Im X(\omega) \sin(\omega n) \, d\omega$$

*except for two special cases:*

$$Re \bar{X}[0] = \frac{Re X[0]}{N}$$

$$Re \bar{X}[N/2] = \frac{Re X[N/2]}{N}$$

$$Re X[k] = \sum_{i=0}^{N-1} x[i] \cos(2\pi k i / N)$$

$$Im X[k] = - \sum_{i=0}^{N-1} x[i] \sin(2\pi k i / N)$$

$$a_n = \frac{2}{T} \int_{-T/2}^{T/2} x(t) \cos\left(\frac{2\pi t n}{T}\right) dt$$

$$b_n = \frac{-2}{T} \int_{-T/2}^{T/2} x(t) \sin\left(\frac{2\pi t n}{T}\right) dt$$

# THE DISCRETE FOURIER TRANSFORM (DFT)

- A Periodic Signal Can be Decomposed into the Sum of Properly Chosen Cosine and Sine Waves (Jean Baptiste Joseph Fourier, 1807)

- The DFT Operates on a Finite Number (N) of Digitized Time Samples, x(n). When These Samples are Repeated and Placed "End-to-End", they Appear Periodic to the Transform.

- The Complex DFT Output Spectrum X(k) is the Result of Correlating the Input Samples with sine and cosine Basis Functions:

$$X(k) = \frac{1}{N}\sum_{n=0}^{N-1} x(n)\, e^{\frac{-j2\pi nk}{N}} = \frac{1}{N}\sum_{n=0}^{N-1} x(n)\left[\cos\frac{2\pi nk}{N} - j\sin\frac{2\pi nk}{N}\right]$$

$$0 \le k \le N-1$$

# CORRELATION OF TIME SAMPLES WITH BASIS FUNCTIONS USING THE DFT FOR N = 8

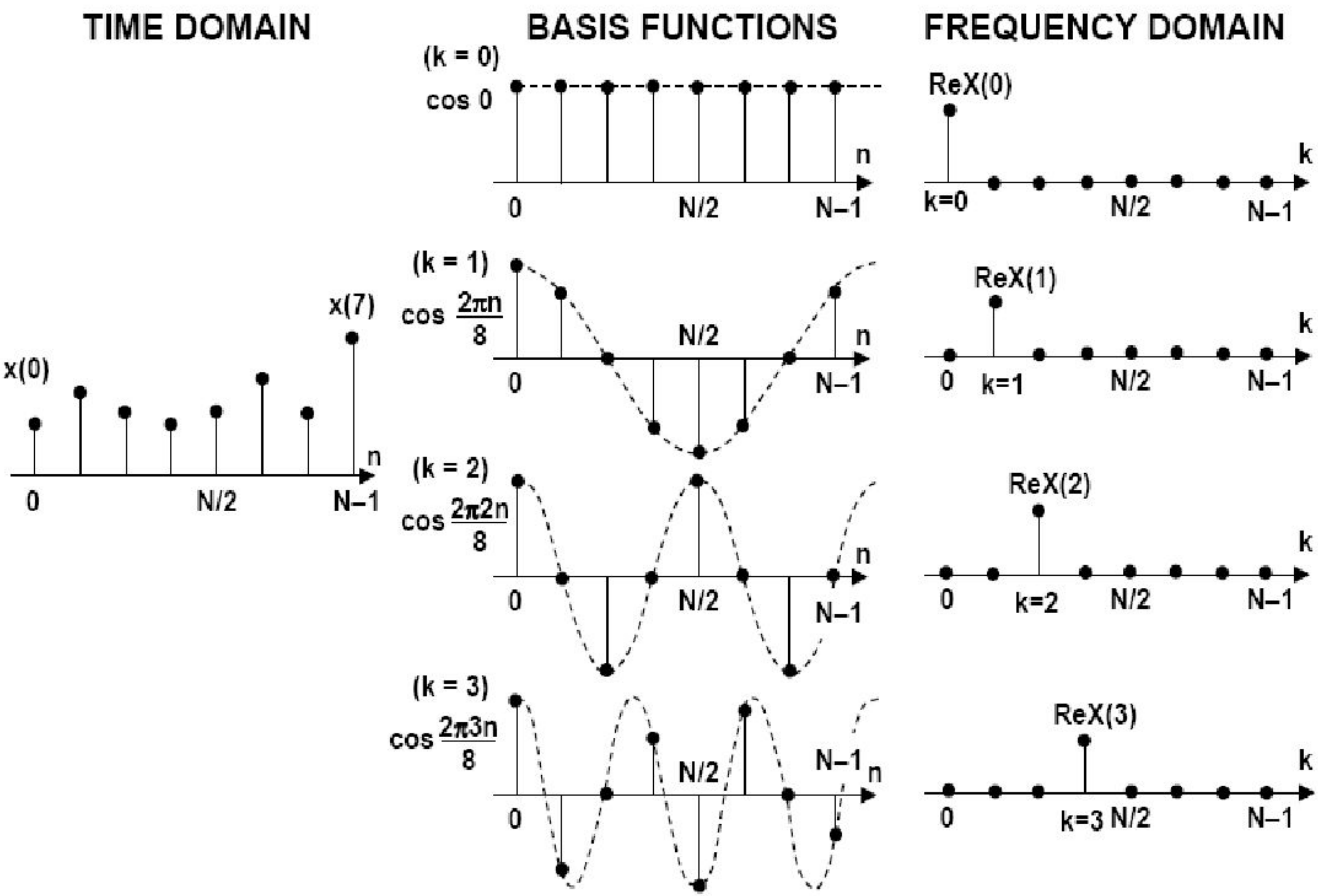

# APPLICATIONS OF THE DISCRETE FOURIER TRANSFORM (DFT)

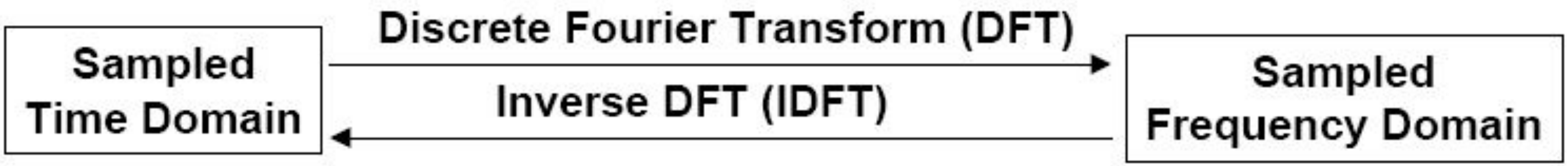


- Digital Spectral Analysis
  - Spectrum Analyzers
  - Speech Processing
  - Imaging
  - Pattern Recognition
- Filter Design
  - Calculating Impulse Response from Frequency Response
  - Calculating Frequency Response from Impulse Response
- The Fast Fourier Transform (FFT) is Simply an Algorithm for Efficiently Calculating the DFT

# FOURIER TRANSFORM FAMILY
# AS A FUNCTION OF TIME DOMAIN SIGNAL TYPE

**FOURIER TRANSFORM:**
Signal is Continuous
and Aperiodic

**FOURIER SERIES:**
Signal is Continuous
and Periodic

**DISCRETE TIME FOURIER SERIES:**
Signal is Sampled
and Aperiodic

**DISCRETE FOURIER TRANSFORM:**
(Discrete Fourier Series)
Signal is Sampled
and Periodic

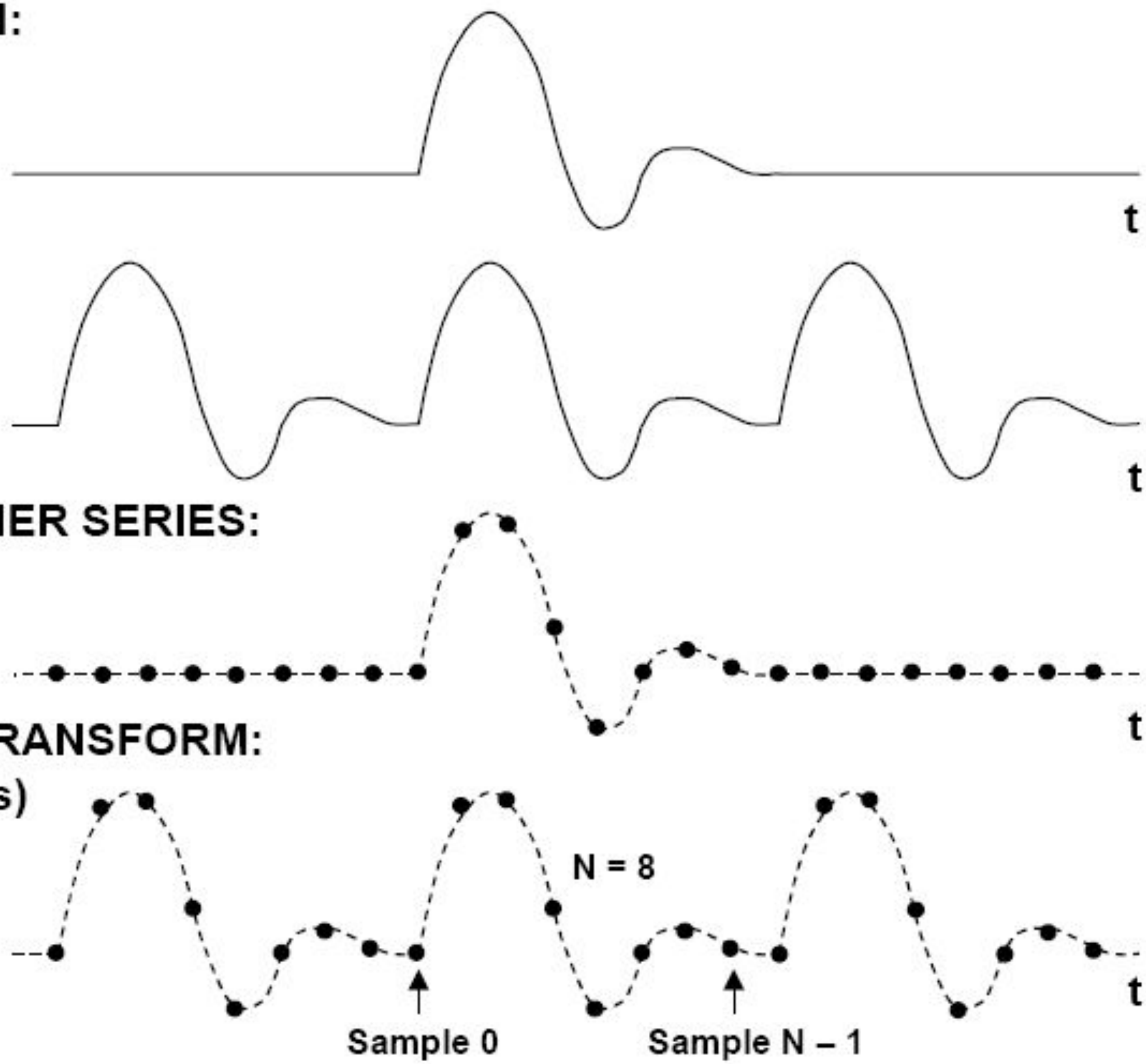

**Frequency Domain ←← DFT ←← Time Domain**

$$X(k) = \frac{1}{N}\sum_{n=0}^{N-1} x(n)\, e^{\frac{-j2\pi nk}{N}} = \frac{1}{N}\sum_{n=0}^{N-1} x(n)\left[\cos\frac{2\pi\, nk}{N} - j\sin\frac{2\pi\, nk}{N}\right]$$

$$W_N = e^{\frac{-j2\pi}{N}}$$

$$= \frac{1}{N}\sum_{n=0}^{N-1} x(n)\, W_N^{nk} \quad , \quad 0 \le k \le N-1$$

**Time Domain ←← INVERSE DFT ←← Frequency Domain**

$$x(n) = \sum_{k=0}^{N-1} X(k)\, e^{\frac{j2\pi nk}{N}} = \sum_{k=0}^{N-1} X(k)\left[\cos\frac{2\pi\, nk}{N} + j\sin\frac{2\pi\, nk}{N}\right]$$

$$= \sum_{k=0}^{N-1} X(k)\, W_N^{-nk} \quad , \quad 0 \le n \le N-1$$

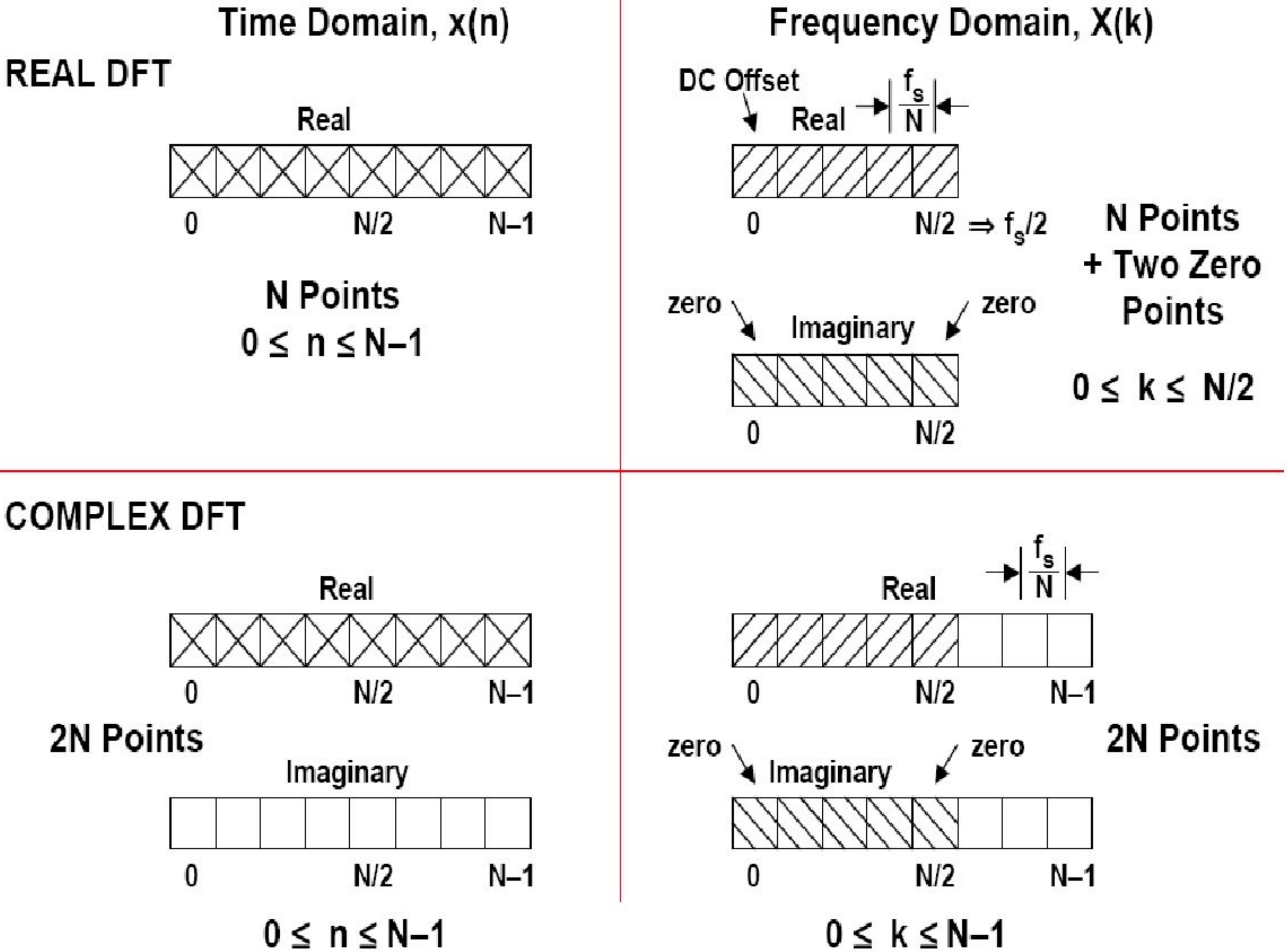
Time Domain, x(n)
Frequency Domain, X(k)
REAL DFT
Real
0
N/2
N–1
N Points
0 ≤ n ≤ N–1
DC Offset
Real
fs/N
0
N/2 ⇒ fs/2
N Points
+ Two Zero
Points
zero
Imaginary
zero
0
N/2
0 ≤ k ≤ N/2
COMPLEX DFT
Real
0
N/2
N–1
2N Points
Imaginary
0
N/2
N–1
0 ≤ n ≤ N–1
Real
fs/N
0
N/2
N–1
2N Points
zero
Imaginary
zero
0
N/2
N–1
0 ≤ k ≤ N–1

# CONSTRUCTING THE COMPLEX DFT NEGATIVE FREQUENCY COMPONENTS FROM THE REAL DFT

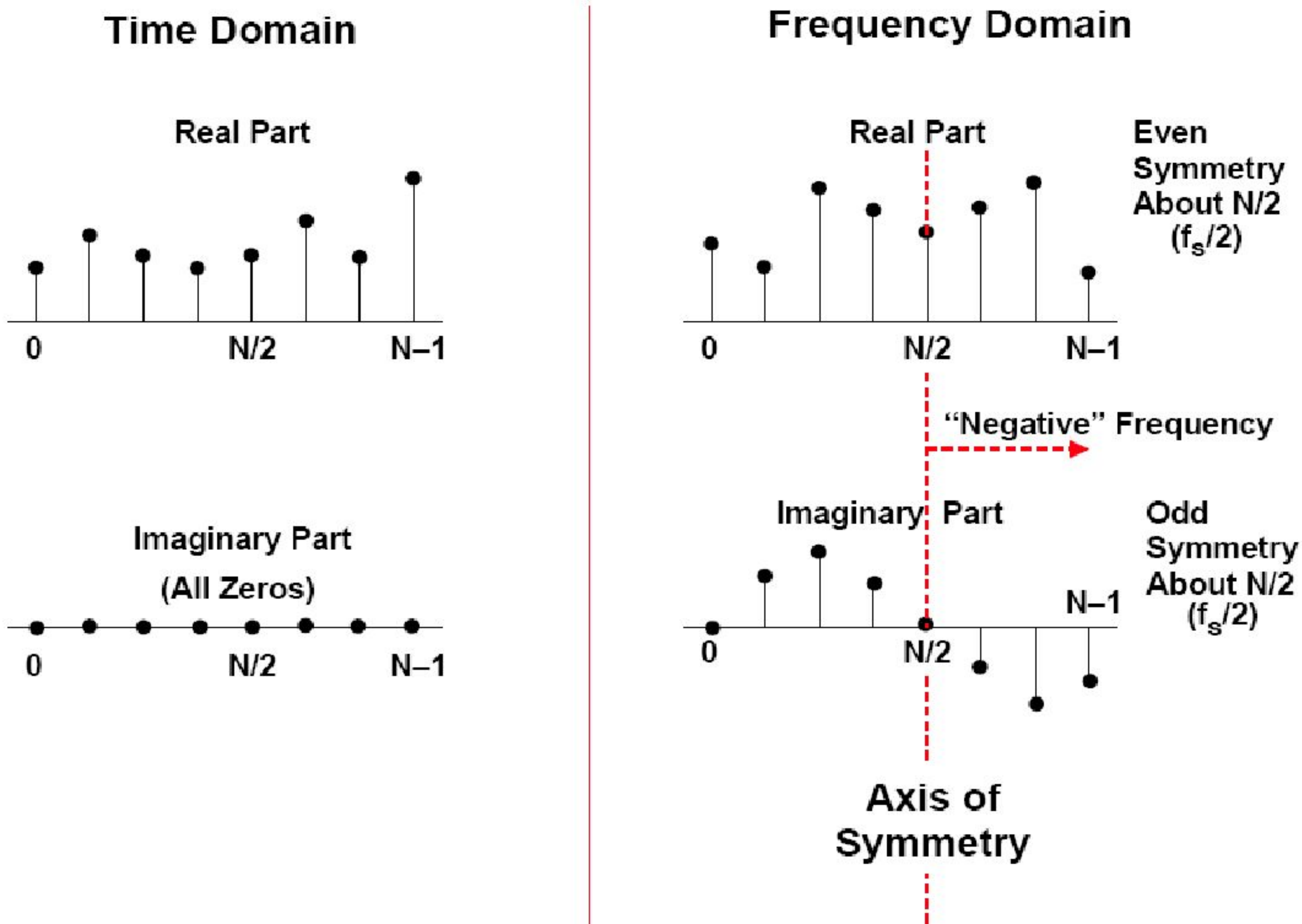

# COMPLEX AND REAL DFT EQUATIONS

## COMPLEX TRANSFORM

$$X(k) = \frac{1}{N} \sum_{n=0}^{N-1} x(n)\, e^{\frac{-j2\pi nk}{N}}$$

$$x(n) = \sum_{k=0}^{N-1} X(k)\, e^{\frac{j2\pi nk}{N}}$$

Time Domain: x(n) is complex, discrete, and periodic. n runs from 0 to N– 1

## REAL TRANSFORM

$$ReX(k) = \frac{2}{N} \sum_{n=0}^{N-1} x(n) \cos(2\pi nk/N)$$

$$ImX(k) = \frac{-2}{N} \sum_{n=0}^{N-1} x(n) \sin(2\pi nk/N)$$

$$x(n) = \sum_{k=0}^{N/2} \left[ ReX(k) \cos(2\pi nk/N) - ImX(k) \cos(2\pi nk/N) \right]$$

Time Domain: x(n) is real, discrete, and periodic. n runs from 0 to N – 1

# THE 8-POINT DFT (N = 8)

$$X(k) = \frac{1}{N}\sum_{n=0}^{N-1} x(n)\, e^{\frac{-j2\pi nk}{N}} = \frac{1}{N}\sum_{n=0}^{N-1} x(n)\, W_N^{nk}$$

$$W_N = e^{\frac{-j2\pi}{N}}$$

| | |
|---|---|
| $X(0) =$ | $x(0)W_8^0 + x(1)W_8^0 + x(2)W_8^0 + x(3)W_8^0 + x(4)W_8^0 + x(5)W_8^0 + x(6)W_8^0 + x(7)W_8^0$ |
| $X(1) =$ | $x(0)W_8^0 + x(1)W_8^1 + x(2)W_8^2 + x(3)W_8^3 + x(4)W_8^4 + x(5)W_8^5 + x(6)W_8^6 + x(7)W_8^7$ |
| $X(2) =$ | $x(0)W_8^0 + x(1)W_8^2 + x(2)W_8^4 + x(3)W_8^6 + x(4)W_8^8 + x(5)W_8^{10} + x(6)W_8^{12} + x(7)W_8^{14}$ |
| $X(3) =$ | $x(0)W_8^0 + x(1)W_8^3 + x(2)W_8^6 + x(3)W_8^9 + x(4)W_8^{12} + x(5)W_8^{15} + x(6)W_8^{18} + x(7)W_8^{21}$ |
| $X(4) =$ | $x(0)W_8^0 + x(1)W_8^4 + x(2)W_8^8 + x(3)W_8^{12} + x(4)W_8^{16} + x(5)W_8^{20} + x(6)W_8^{24} + x(7)W_8^{28}$ |
| $X(5) =$ | $x(0)W_8^0 + x(1)W_8^5 + x(2)W_8^{10} + x(3)W_8^{15} + x(4)W_8^{20} + x(5)W_8^{25} + x(6)W_8^{30} + x(7)W_8^{35}$ |
| $X(6) =$ | $x(0)W_8^0 + x(1)W_8^6 + x(2)W_8^{12} + x(3)W_8^{18} + x(4)W_8^{24} + x(5)W_8^{30} + x(6)W_8^{36} + x(7)W_8^{42}$ |
| $X(7) =$ | $x(0)W_8^0 + x(1)W_8^7 + x(2)W_8^{14} + x(3)W_8^{21} + x(4)W_8^{28} + x(5)W_8^{35} + x(6)W_8^{42} + x(7)W_8^{49}$ |

$N^2$ Complex Multiplications

$\frac{1}{N}$ Scaling Factor Omitted

# APPLYING THE PROPERTIES OF SYMMETRY AND PERIODICITY TO $W_N^r$ FOR N = 8

Symmetry: $W_N^{r+N/2} = -W_N^r$ , Periodicity: $W_N^{r+N} = W_N^r$

N = 8

$$W_8^4 = W_8^{0+4} = -W_8^0 = -1$$
$$W_8^5 = W_8^{1+4} = -W_8^1$$
$$W_8^6 = W_8^{2+4} = -W_8^2$$
$$W_8^7 = W_8^{3+4} = -W_8^3$$
$$W_8^8 = W_8^{0+8} = +W_8^0 = +1$$
$$W_8^9 = W_8^{1+8} = +W_8^1$$
$$W_8^{10} = W_8^{2+8} = +W_8^2$$
$$W_8^{11} = W_8^{3+8} = +W_8^3$$

$$\vdots \qquad \vdots \qquad \vdots$$

# THE FAST FOURIER TRANSFORM (FFT) VS. THE DISCRETE FOURIER TRANSFORM (DFT)

- The FFT is Simply an Algorithm for Efficiently Calculating the DFT
- Computational Efficiency of an N-Point FFT:
  - DFT: $N^2$ Complex Multiplications
  - FFT: $(N/2) \log_2(N)$ Complex Multiplications

| N | DFT Multiplications | FFT Multiplications | FFT Efficiency |
|---|---|---|---|
| 256 | 65,536 | 1,024 | 64 : 1 |
| 512 | 262,144 | 2,304 | 114 : 1 |
| 1,024 | 1,048,576 | 5,120 | 205 : 1 |
| 2,048 | 4,194,304 | 11,264 | 372 : 1 |
| 4,096 | 16,777,216 | 24,576 | 683 : 1 |

## THE BASIC BUTTERFLY COMPUTATION IN THE DECIMATION-IN-TIME FFT ALGORITHM

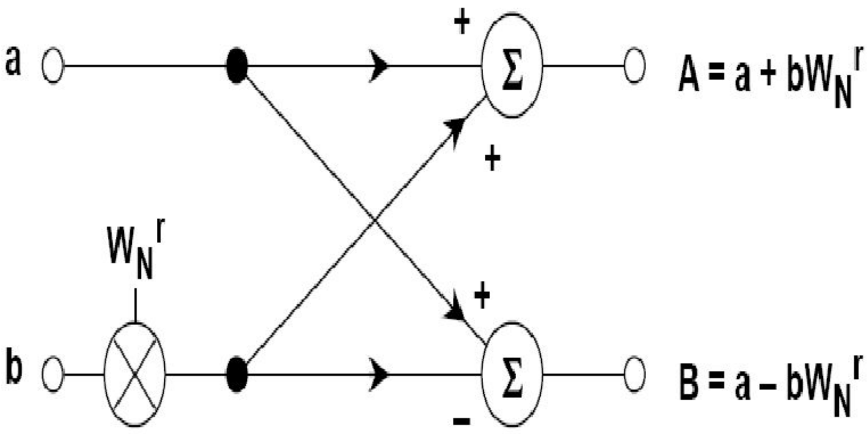


SIMPLIFIED REPRESENTATION

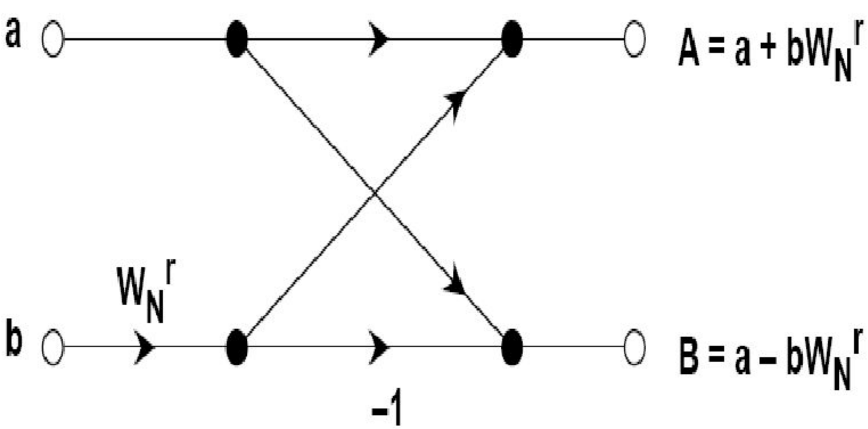


## THE BASIC BUTTERFLY COMPUTATION IN THE DECIMATION-IN-FREQUENCY FFT ALGORITHM

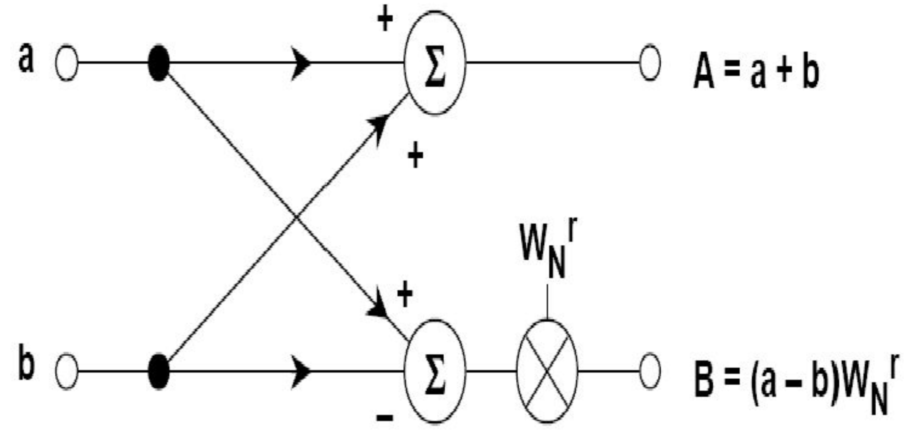


SIMPLIFIED REPRESENTATION

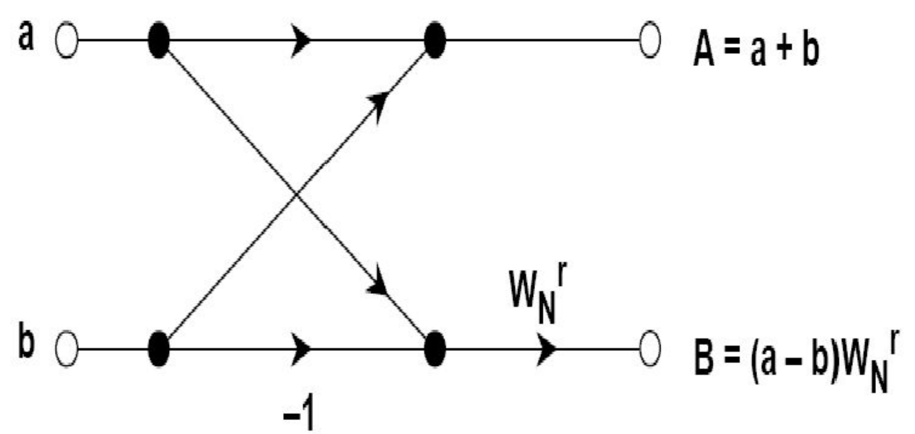

# RADIX-4 FFT DECIMATION-IN-TIME BUTTERFLY

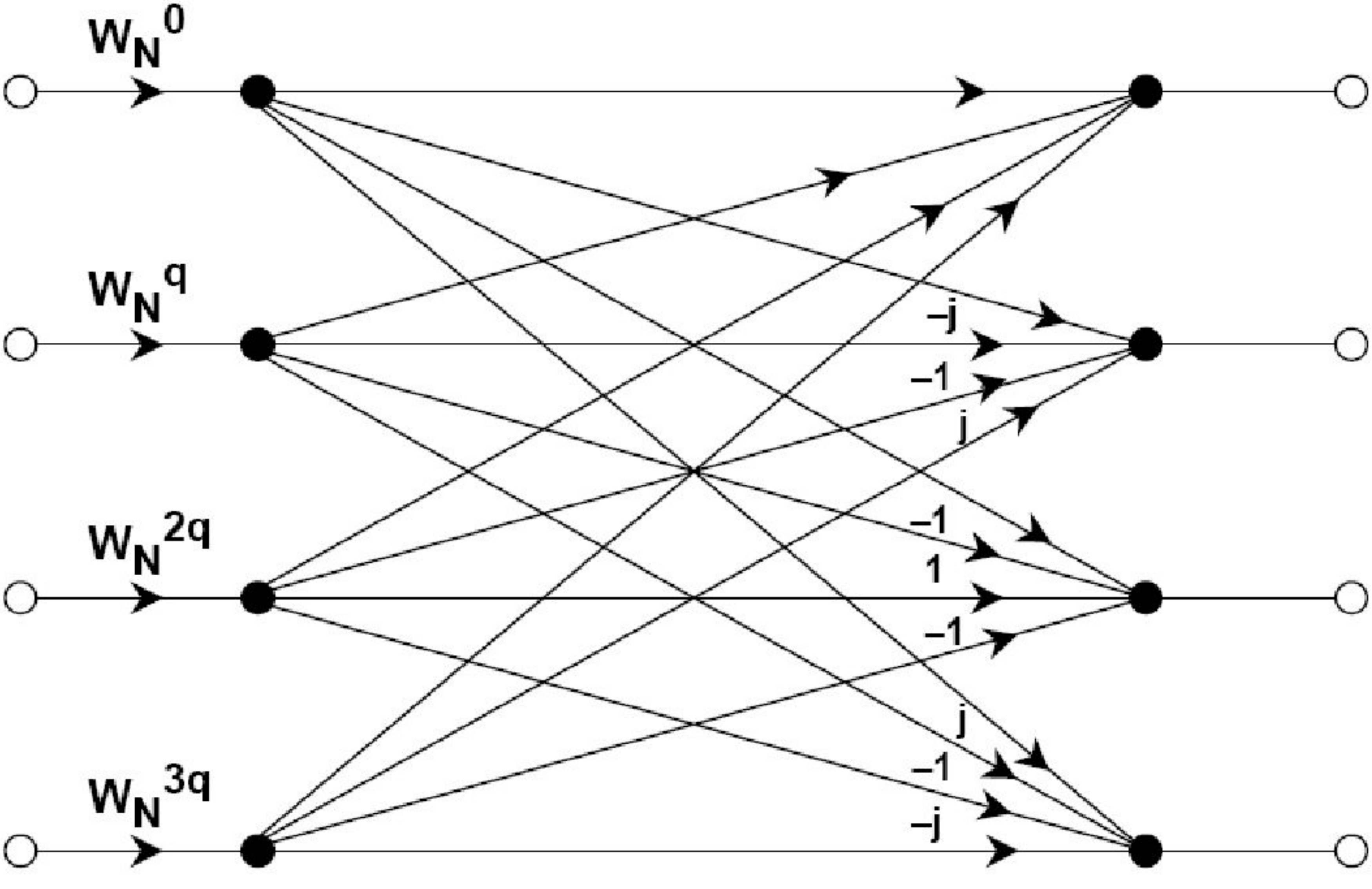

# COMPUTATION OF AN 8-POINT DFT IN THREE STAGES USING DECIMATION-IN-TIME

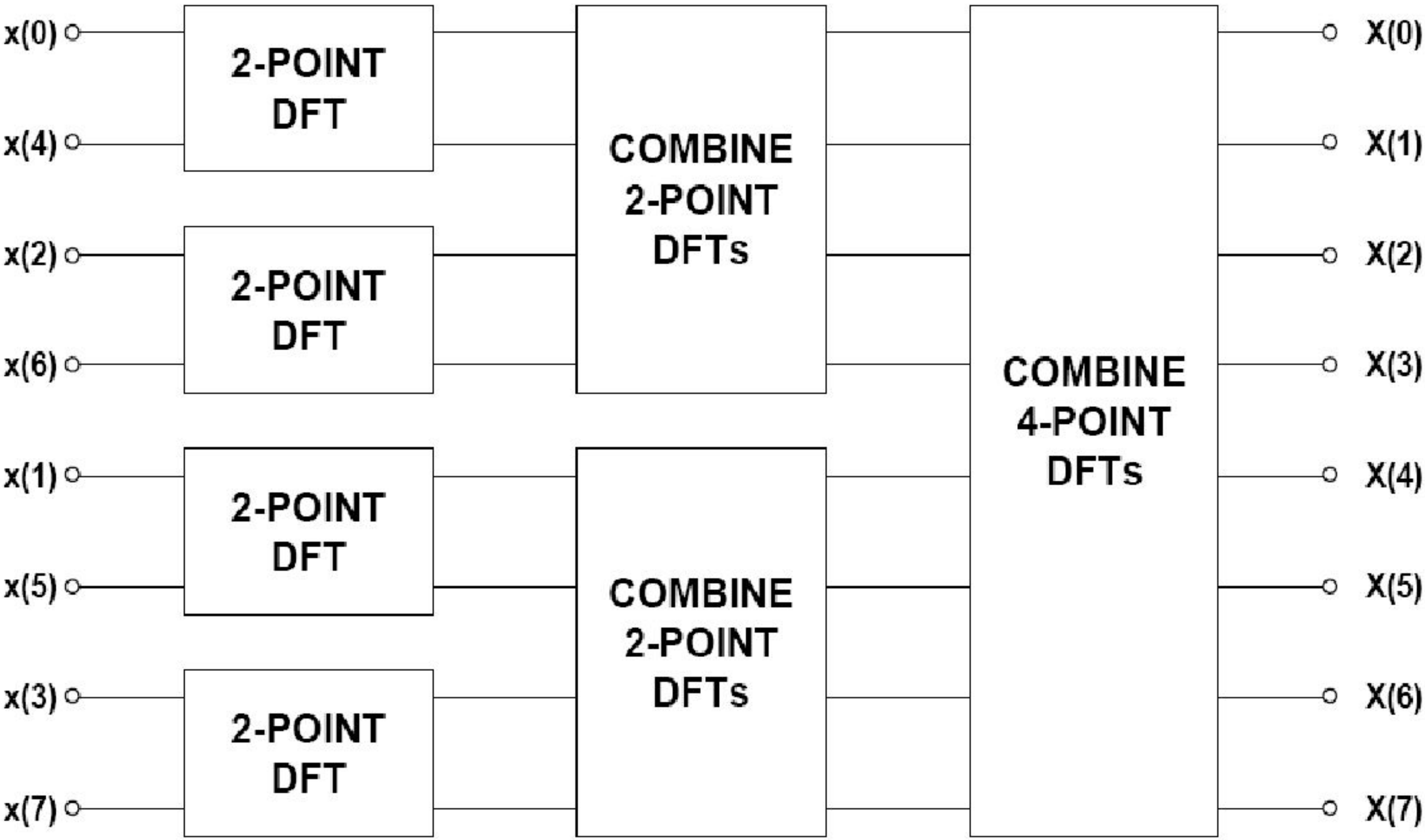

# EIGHT-POINT DECIMATION-IN-TIME FFT ALGORITHM

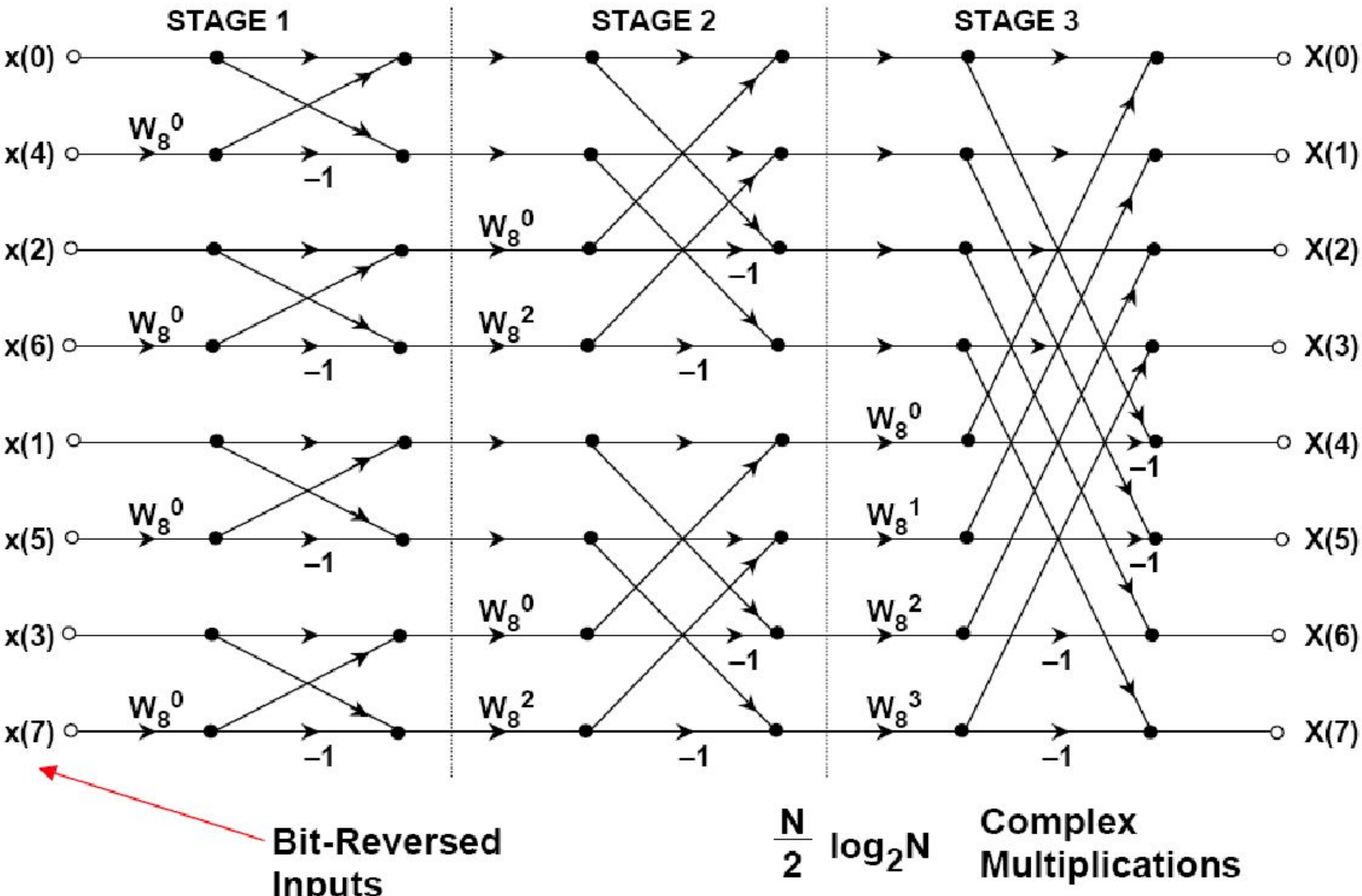


$\frac{N}{2} \log_2 N$ Complex Multiplications

# COMPUTATION OF AN 8-POINT DFT IN THREE STAGES USING DECIMATION-IN-FREQUENCY

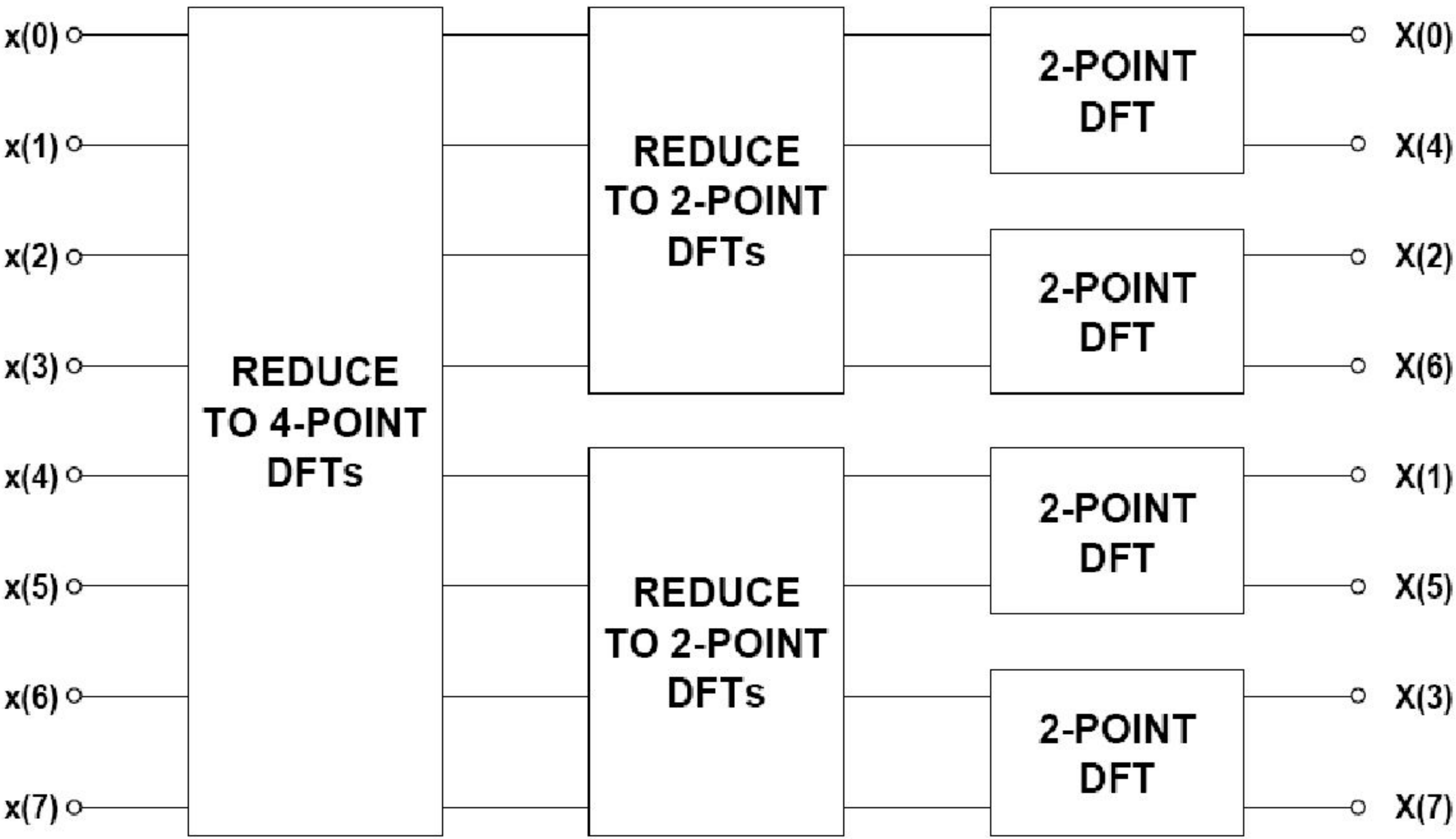

# EIGHT-POINT DECIMATION-IN-FREQUENCY FFT ALGORITHM

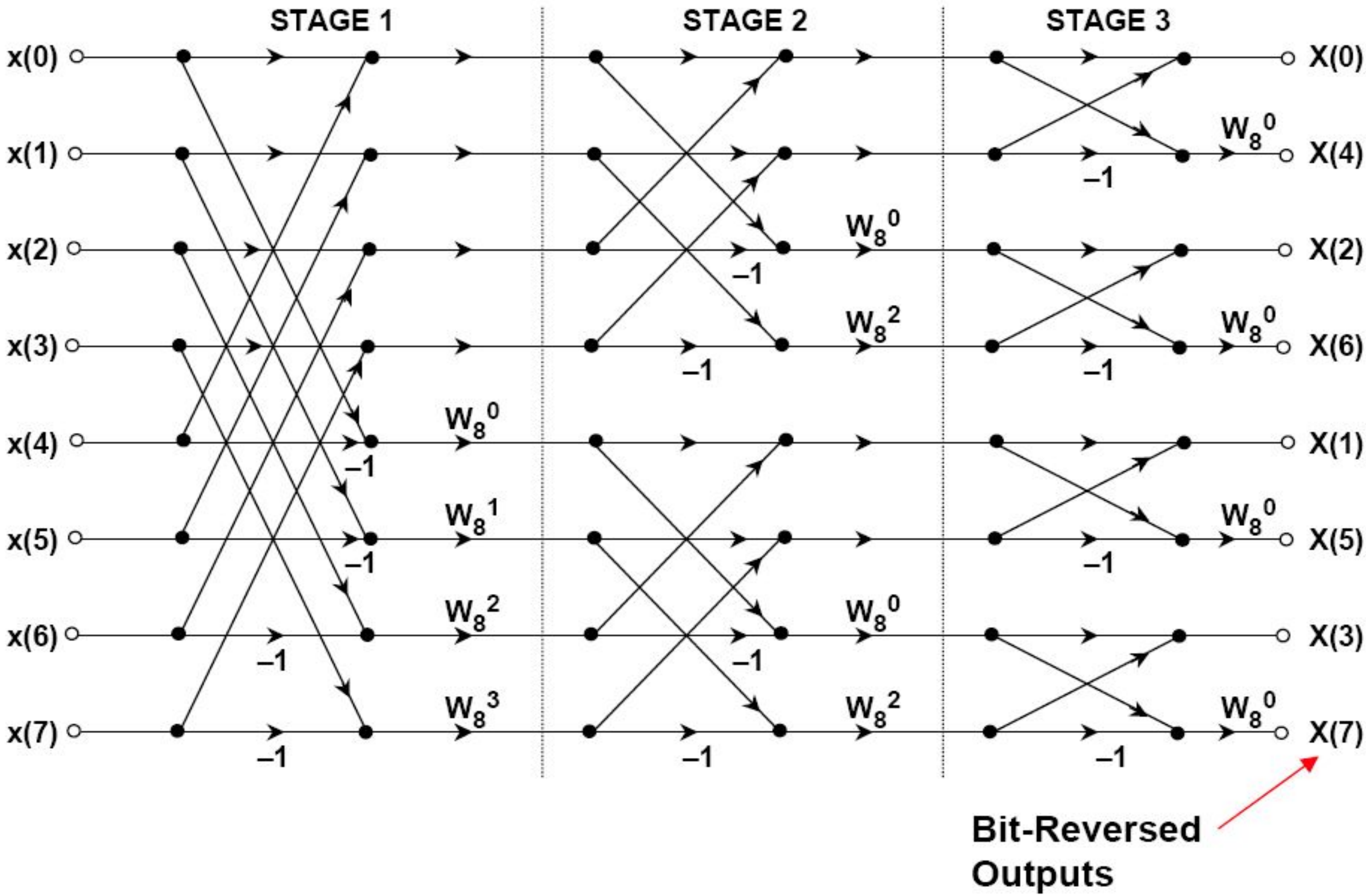

# RADIX-2 COMPLEX FFT HARDWARE BENCHMARK COMPARISONS

- ADSP-2189M, 16-bit, Fixed-Point @ 75MHz
  - 453µs (1024-Point)
- ADSP-21160 SHARC™, 32-bit, Floating-Point @ 100MHz
  - 180µs (1024-Point), 2 channels, SIMD Mode
  - 115µs (1024-Point), 1 channel, SIMD Mode
- ADSP-TS001 TigerSHARC™ @ 150MHz,
  - 16-bit, Fixed-Point Mode
    - 7.3µs (256-Point FFT)
  - 32-bit, Floating-Point Mode
    - 69µs (1024-Point)

# REAL-TIME FFT PROCESSING EXAMPLE

- Assume 69µs Execution Time for Radix-2, 1024-point FFT (TigerSHARC, 32-bit Mode)
- $f_s$ (maximum) < $\dfrac{\text{1024 Samples}}{69\mu s}$ = 14.8MSPS
- Therefore Input Signal Bandwidth < 7.4MHz
- This Assumes No Additional FFT Overhead and No Input/Output Data Transfer Limitations

# REAL TIME FFT CONSIDERATIONS

- Signal Bandwidth
- Sampling Frequency, $f_s$
- Number of Points in FFT, N
- Frequency Resolution = $f_s$ / N
- Maximum Time to Calculate N-Point FFT = N / $f_s$
- Fixed-Point vs. Floating Point DSP
- Radix-2 vs. Radix-4 Execution Time
- FFT Processing Gain = 10 $\log_{10}$(N / 2)
- Windowing Requirements

# FFT PROCESSING GAIN
# NEGLECTING ROUND OFF ERROR

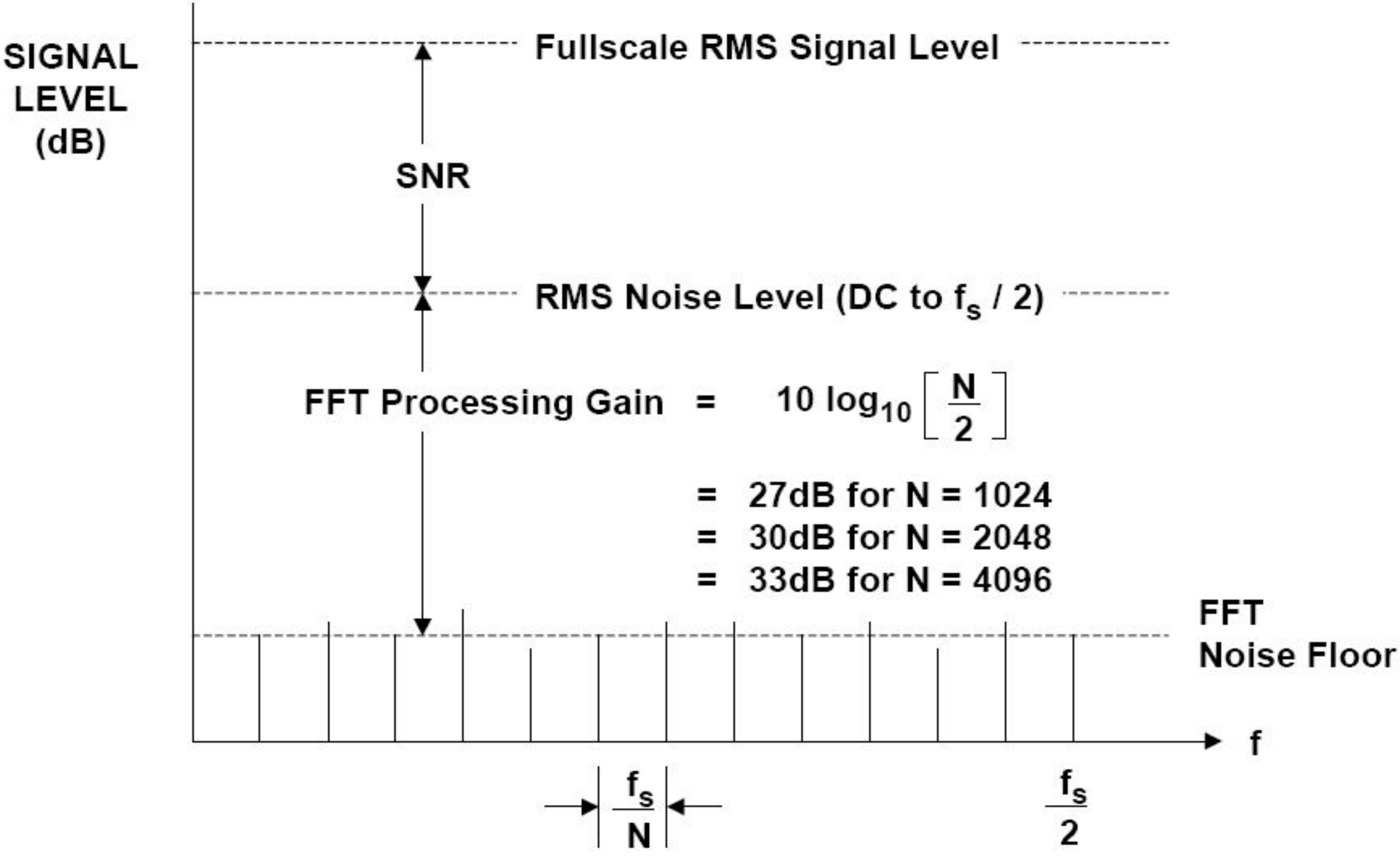

# FFT OF SINEWAVE HAVING INTEGRAL NUMBER OF CYCLES IN DATA WINDOW

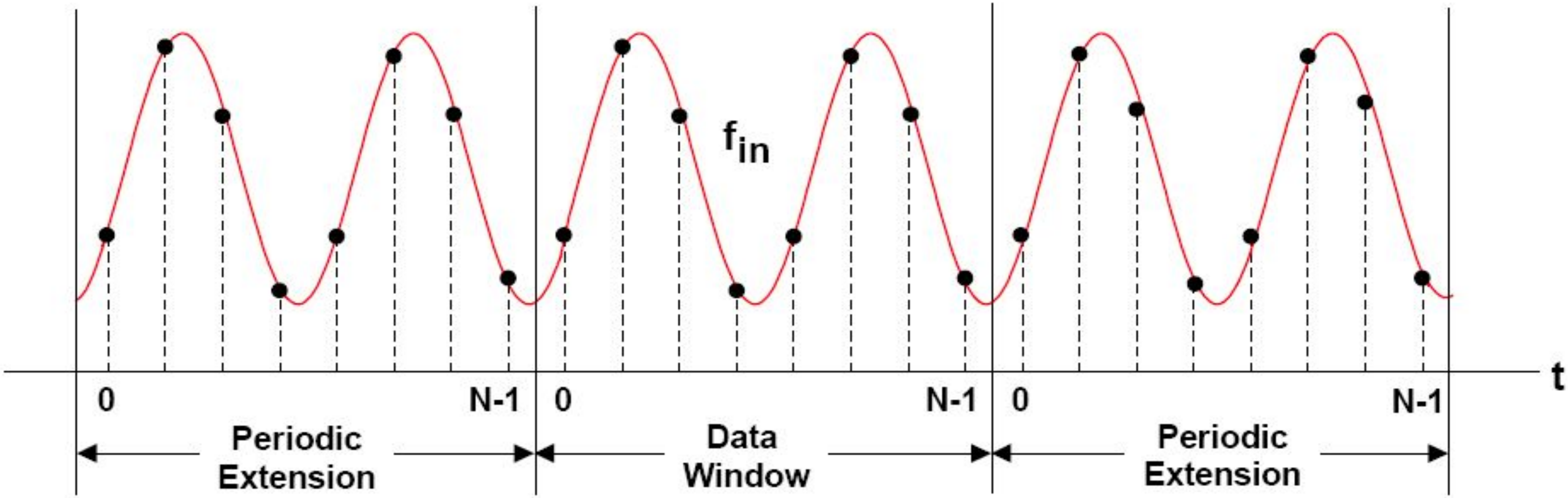


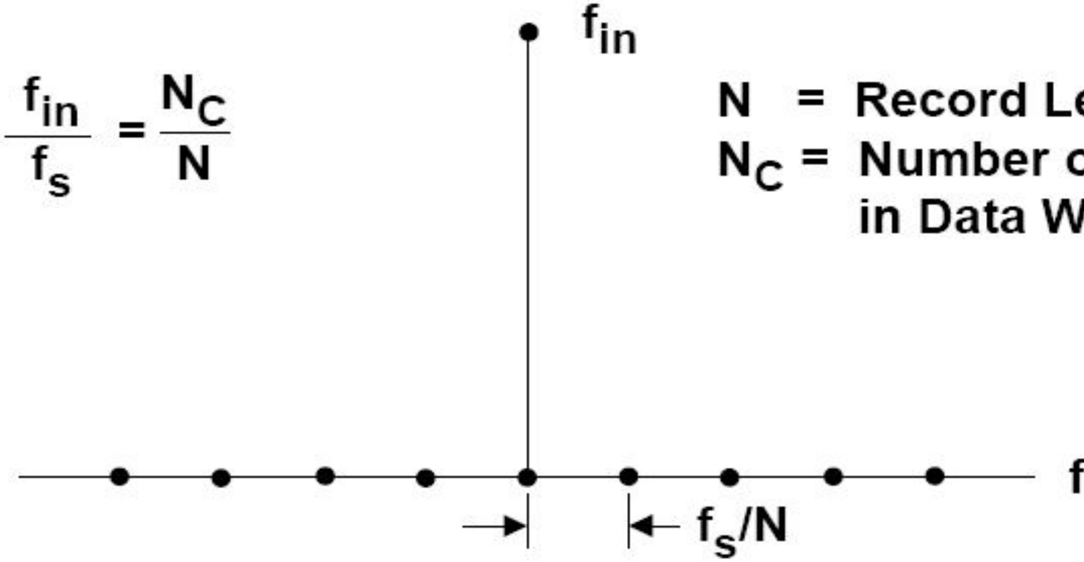


$$\frac{f_{in}}{f_s} = \frac{N_C}{N}$$

N = Record Length

$N_C$ = Number of Cycles in Data Window

# FFT OF SINEWAVE HAVING NON-INTEGRAL NUMBER OF CYCLES IN DATA WINDOW

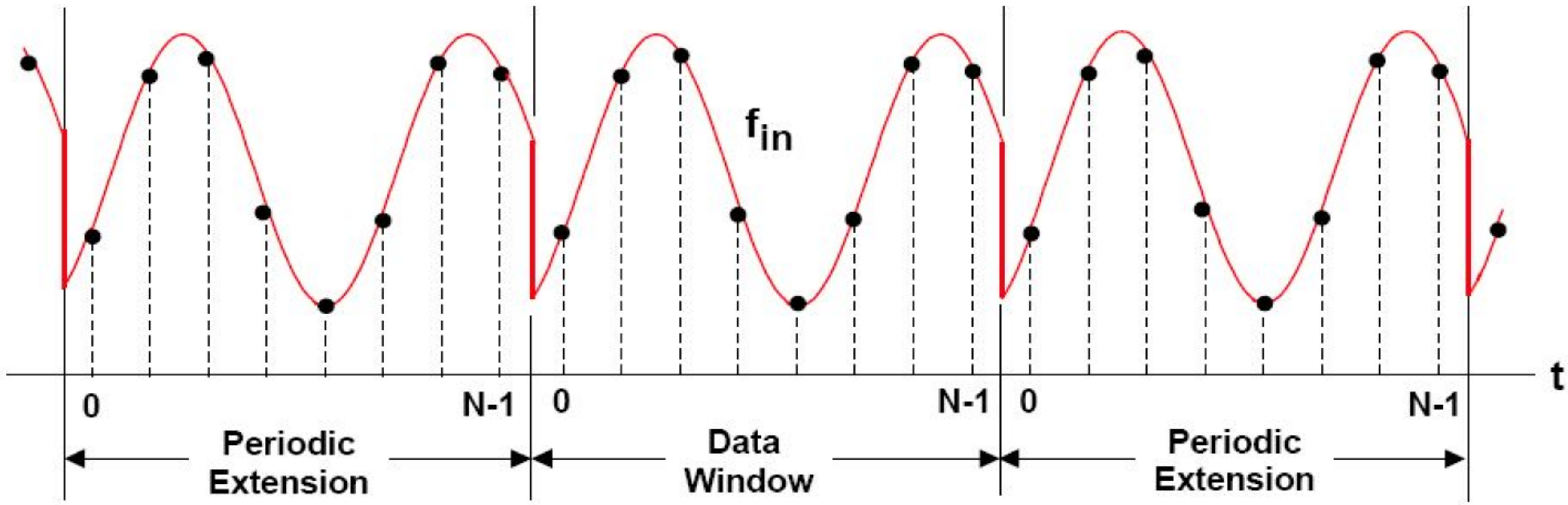


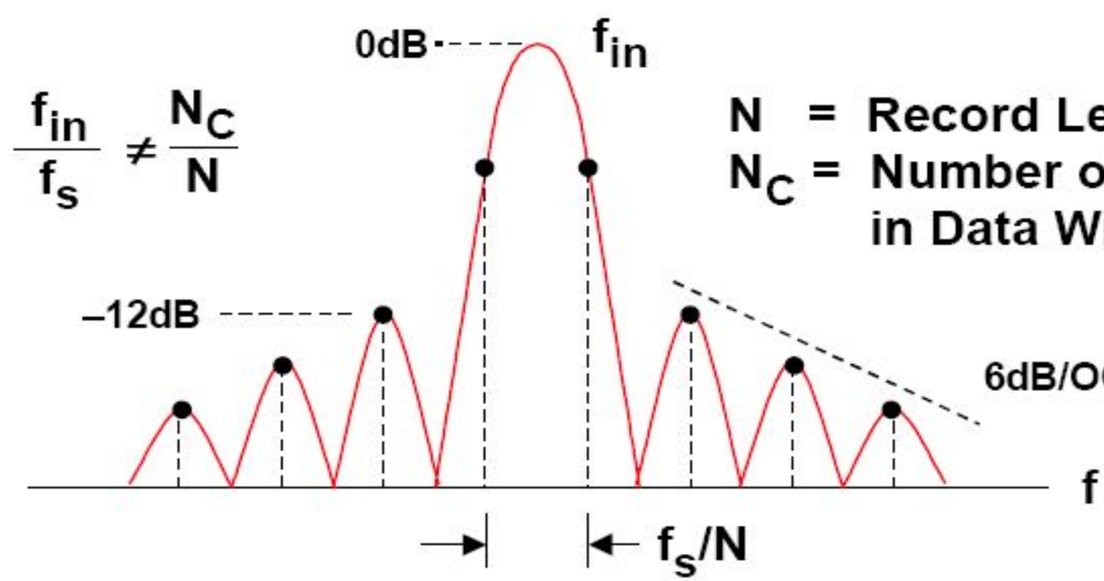

# WINDOWING TO REDUCE SPECTRAL LEAKAGE

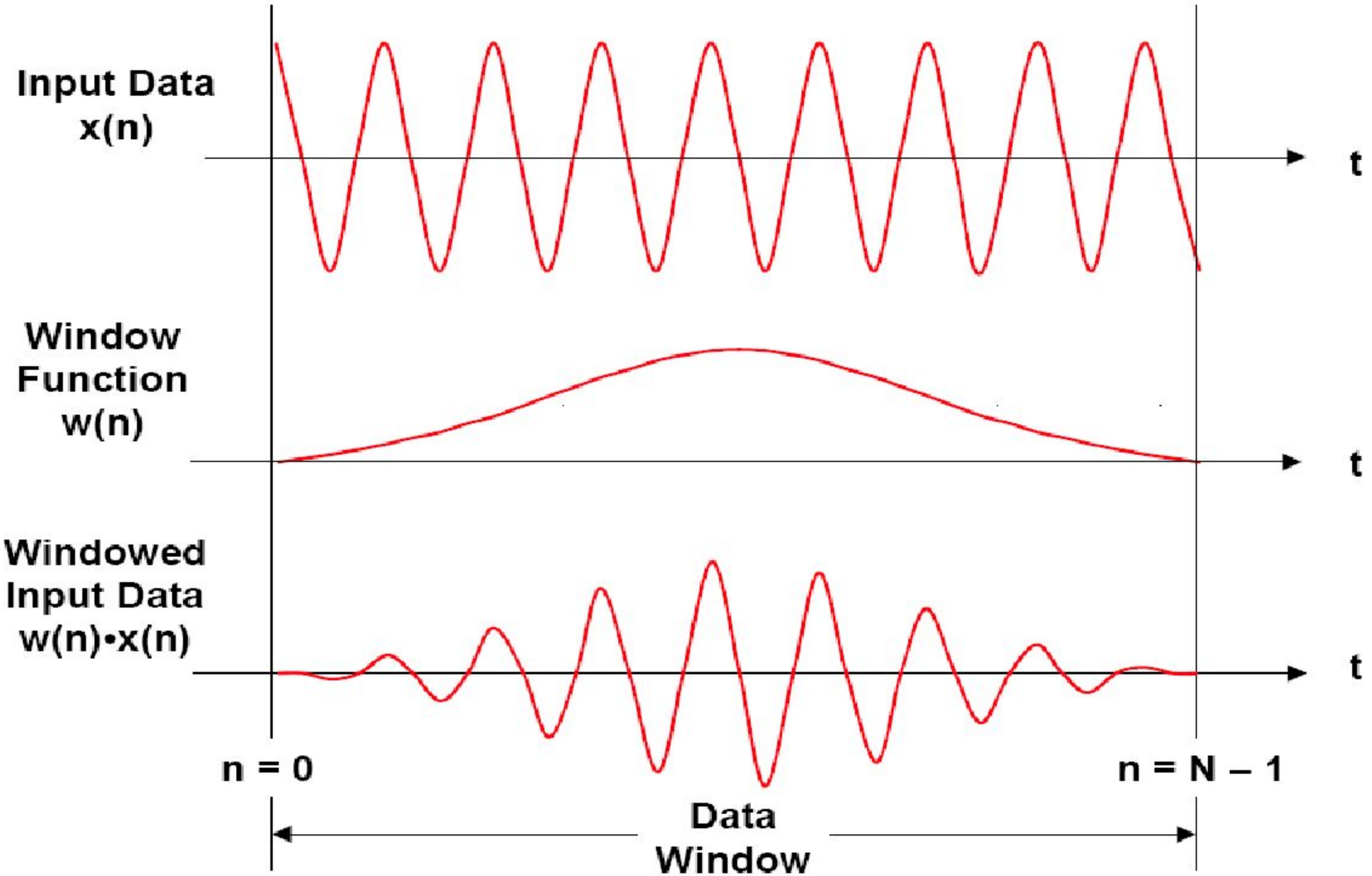

# SOME POPULAR WINDOW FUNCTIONS

- Hamming: $w(n) = 0.54 - 0.46 \cos\left[\frac{2\pi n}{N}\right]$

- Blackman: $w(n) = 0.42 - 0.5 \cos\left[\frac{2\pi n}{N}\right] + 0.08 \cos\left[\frac{4\pi n}{N}\right]$

- Hanning: $w(n) = 0.5 - 0.5 \cos\left[\frac{2\pi n}{N}\right]$

- Minimum 4-Term Blackman Harris: $w(n) = 0.35875 - 0.48829 \cos\left[\frac{2\pi n}{N}\right] + 0.14128 \cos\left[\frac{4\pi n}{N}\right] - 0.01168 \cos\left[\frac{6\pi n}{N}\right]$

$0 \leq n \leq N - 1$

# FREQUENCY RESPONSE OF RECTANGULAR, HAMMING, AND BLACKMAN WINDOWS FOR N = 256

**RECTANGULAR**

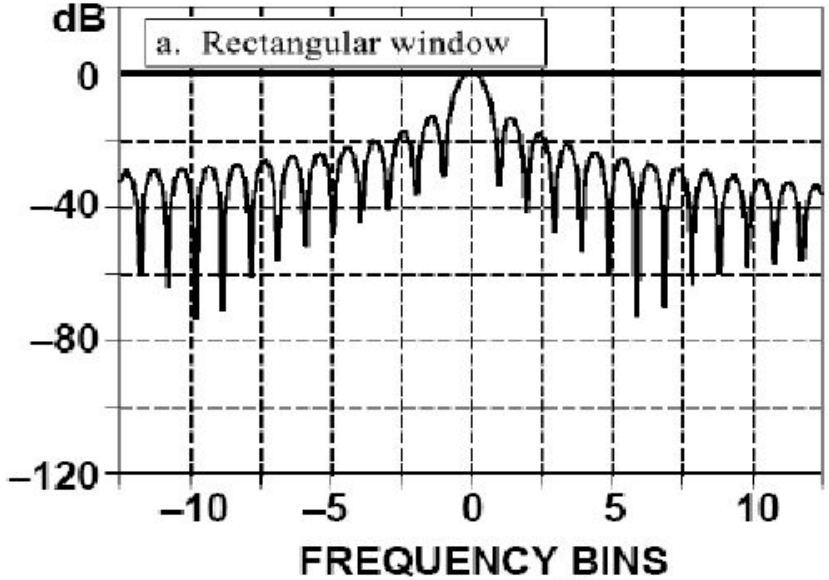


$$\text{BIN WIDTH} = \frac{f_s}{N}$$

**HAMMING**

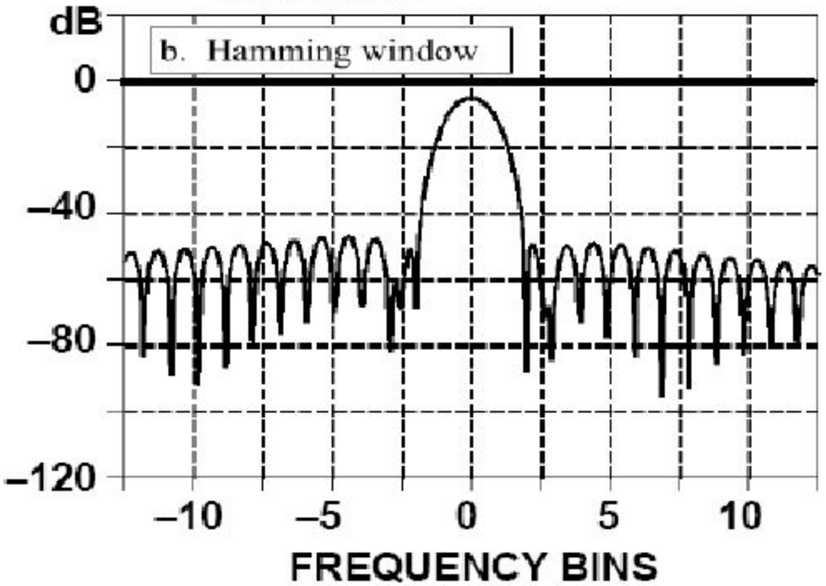


**BLACKMAN**

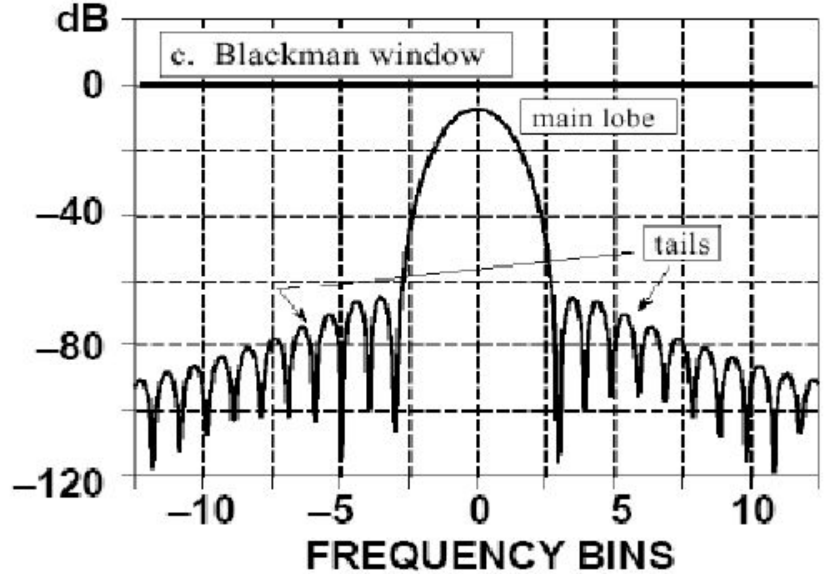

# POPULAR WINDOWS AND FIGURES OF MERIT

| WINDOW FUNCTION | 3dB BW (Bins) | 6dB BW (Bins) | HIGHEST SIDELOBE (dB) | SIDELOBE ROLLOFF (dB/Octave) |
|---|---|---|---|---|
| Rectangle | 0.89 | 1.21 | –12 | 6 |
| Hamming | 1.3 | 1.81 | – 43 | 6 |
| Blackman | 1.68 | 2.35 | –58 | 18 |
| Hanning | 1.44 | 2.00 | –32 | 18 |
| Minimum 4-Term Blackman-Harris | 1.90 | 2.72 | –92 | 6 |

# Примеры Фурье преобразований

**TABLE 5.1. Radial Fourier Transforms of Elementary Signals**

| Signal Expression | Radial Fourier Transform |
|---|---|
| $f(t)$ | $F(\omega) = \int_{-\infty}^{\infty} f(t) e^{-j\omega t} dt$ |
| Square pulse: $u(t+a) - u(t-a)$ | $2a\left[\frac{\sin(\omega a)}{\omega a}\right] = 2a\,\mathrm{sinc}(\omega a)$ |
| Decaying exponential: $e^{-\alpha t}u(t),\ \alpha > 0$ | $\frac{1}{\alpha + j\omega}$ |
| Gaussian: $e^{-\alpha t^2},\ \alpha > 0$ | $\sqrt{\frac{\pi}{\alpha}}e^{\frac{-\omega^2}{4\alpha}}$ |

# Преобразовани Фурье

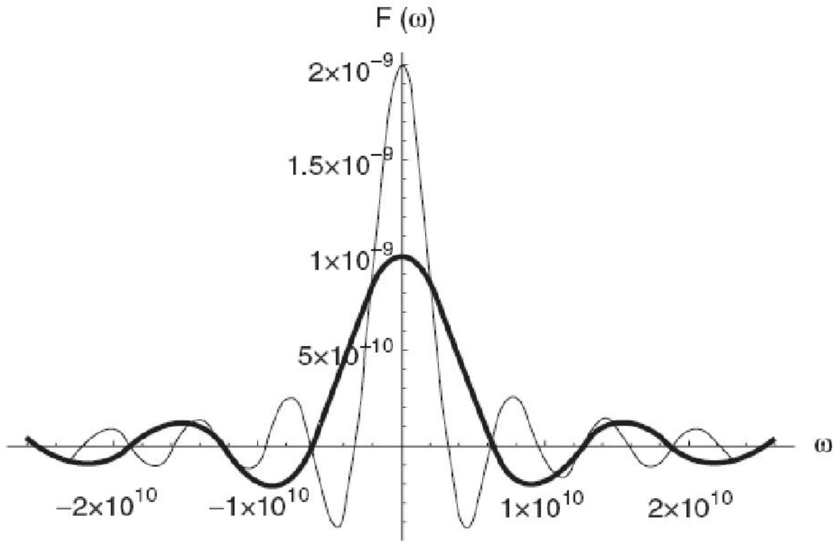


**Fig. 5.5.** The spectrum for a 1-ns rectangular pulse (solid line), and a 2-ns pulse. Note the inverse relationship between pulse width in time and the spread of the frequency spectrum.

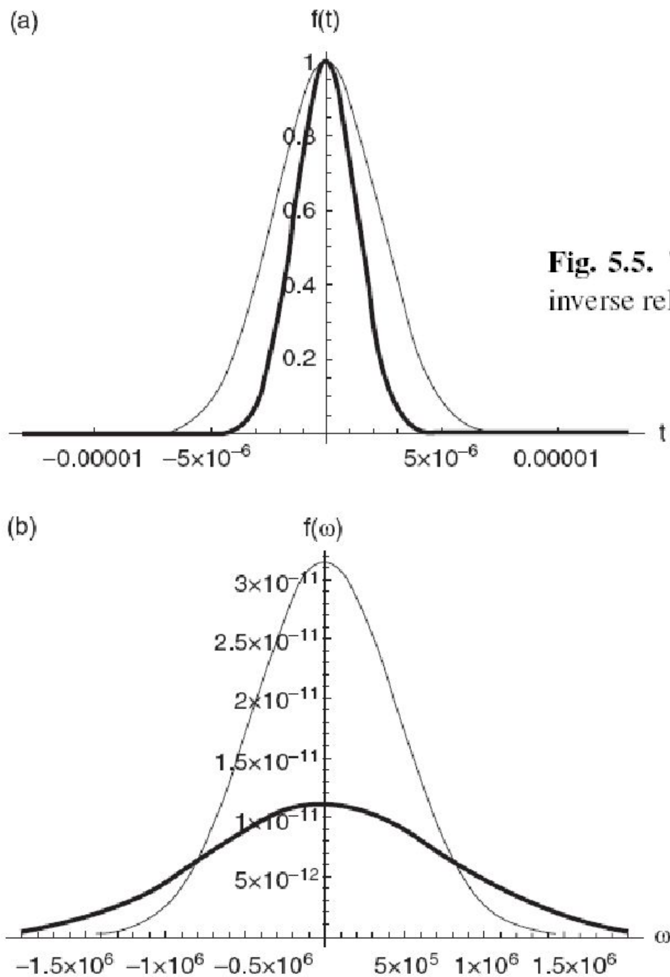


**Fig. 5.7.** (a) Gaussian pulses in the time domain, for $\alpha = 10^{11}$ and $\alpha = 11^{11}$ (solid lines). (b) Corresponding Fourier transforms.

$$f(t) = e^{-\alpha t^2}$$

$$F(\omega) = \int_{-\infty}^{\infty} e^{-\alpha t^2}[\cos(\omega t) - j\sin(\omega t)]\, dt\,.$$

$$F(\omega) = \int_{-\infty}^{\infty} e^{-\alpha t^2}\cos(\omega t)dt = \sqrt{\frac{\pi}{\alpha}}e^{\frac{-\omega^2}{4\alpha}}\,.$$

# Время преобразования

FIGURE 18-3
Execution times for FFT convolution. FFT convolution is faster than the standard method when the filter kernel is longer than about 60 points. These execution times are for a 100 MHz Pentium, using single precision floating point.

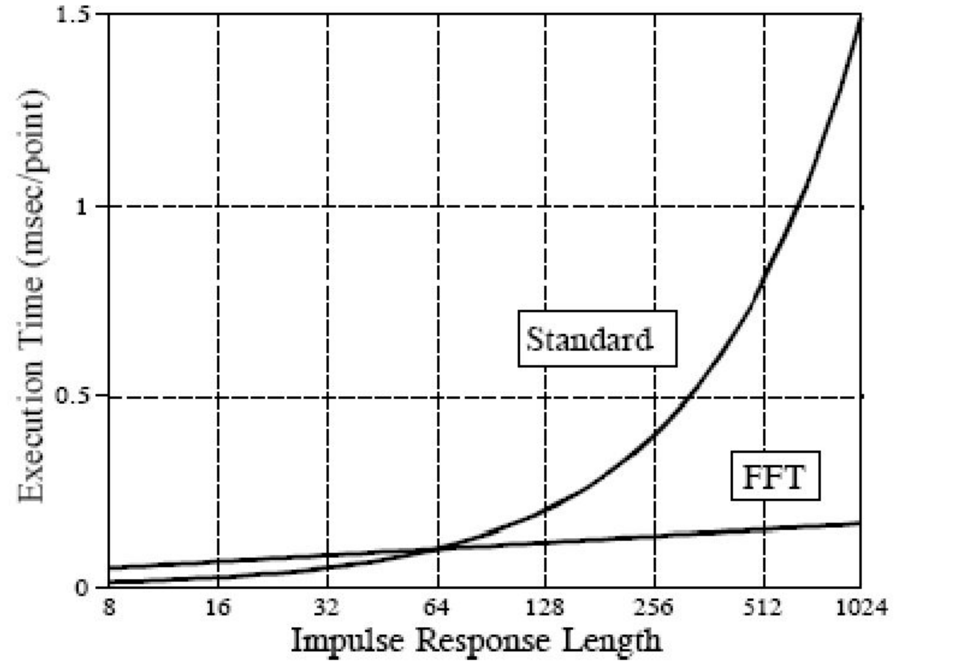


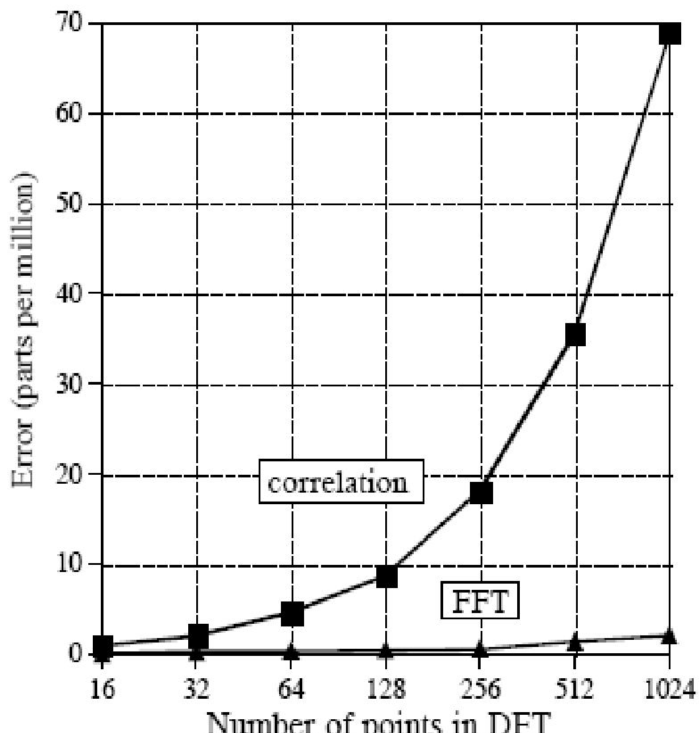


$$ExecutionTime = k_{DFT} N^2$$

$$ExecutionTime = k_{FFT} N \log_2 N$$

# Время преобразования

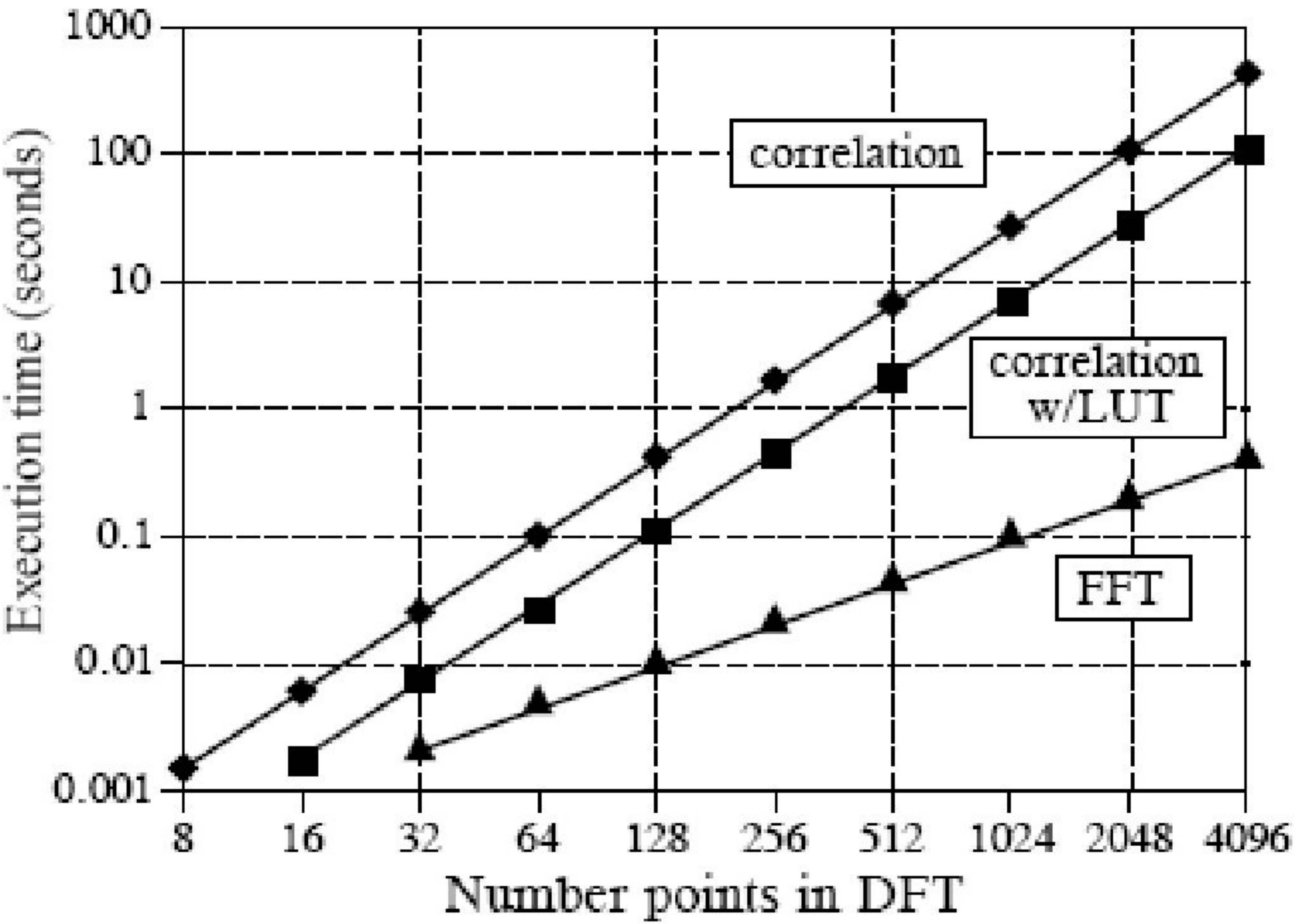

# Бабочка БПФ и шумы округления

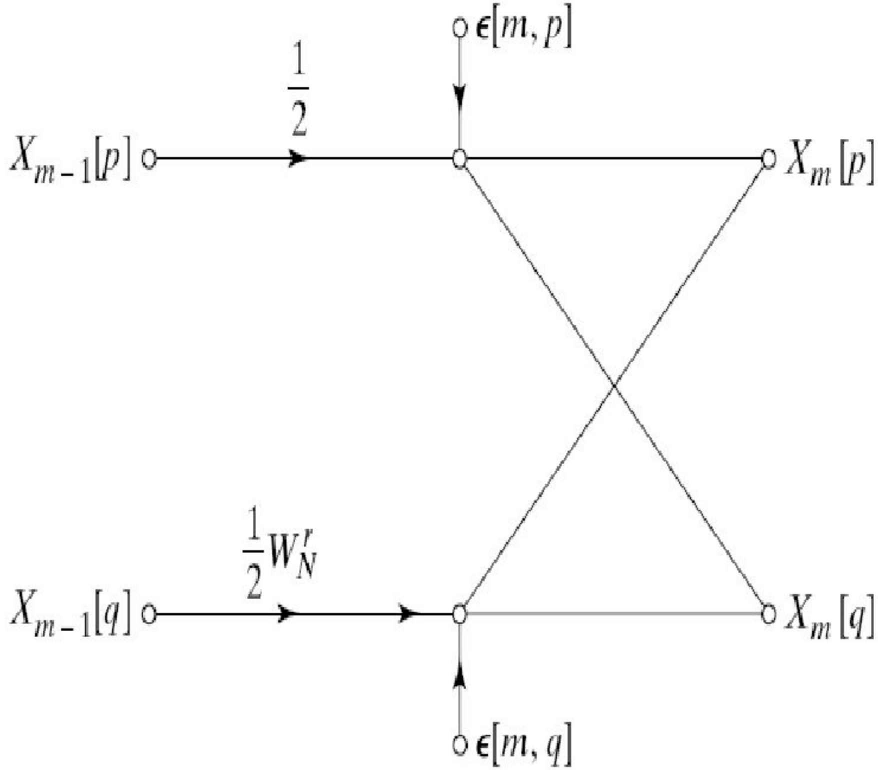


**Figure 9.36** Butterfly showing scaling multipliers and associated fixed- point round-off noise.

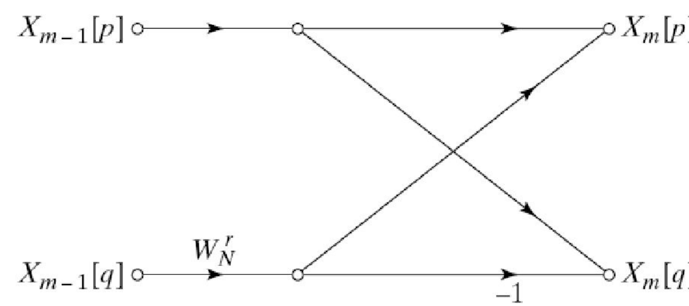


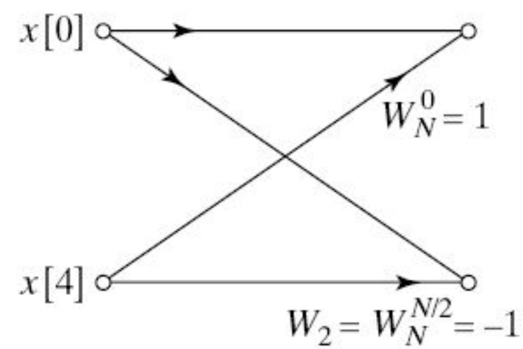


**Figure 9.6** Flow graph of a 2-point DFT.

# БПФ с прореживанием по времени

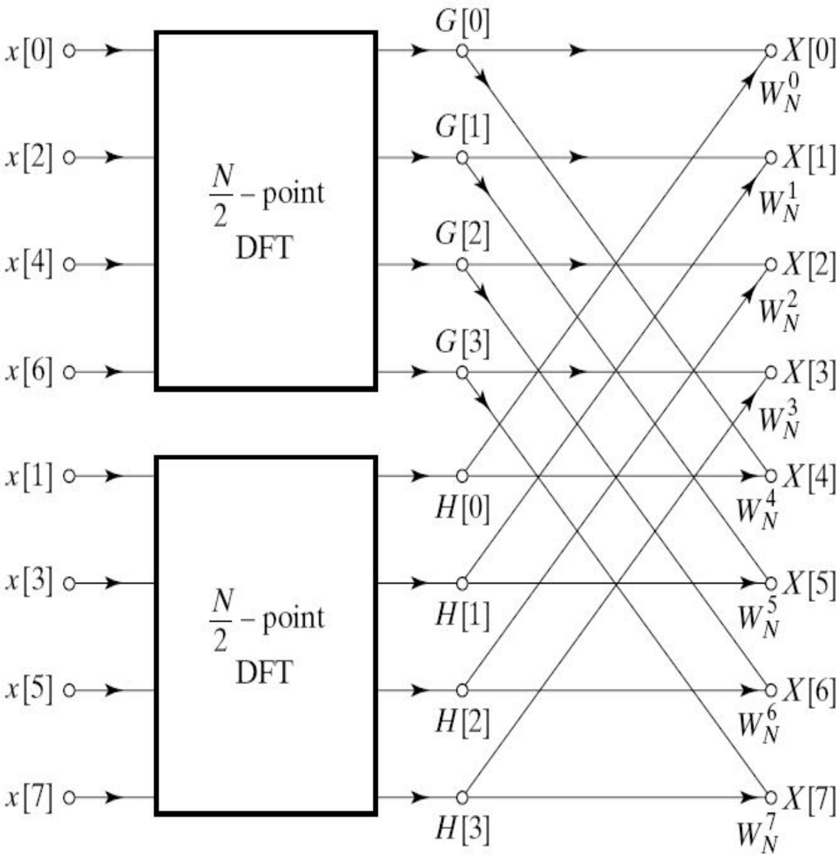


**Figure 9.3** Flow graph of the decimation-in-time decomposition of an $N$-point DFT computation into two ($N/2$)-point DFT computations ($N = 8$).

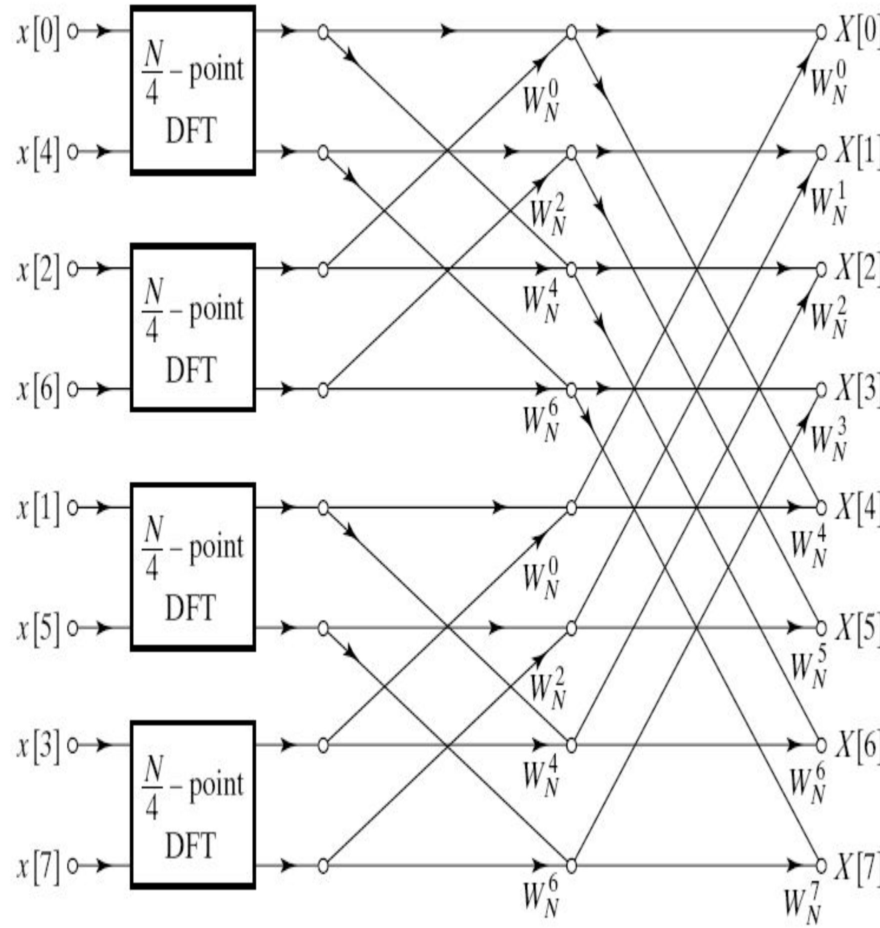


**Figure 9.5** Result of substituting the structure of Figure 9.4 into Figure 9.3.

# БПФ с прореживанием по частоте

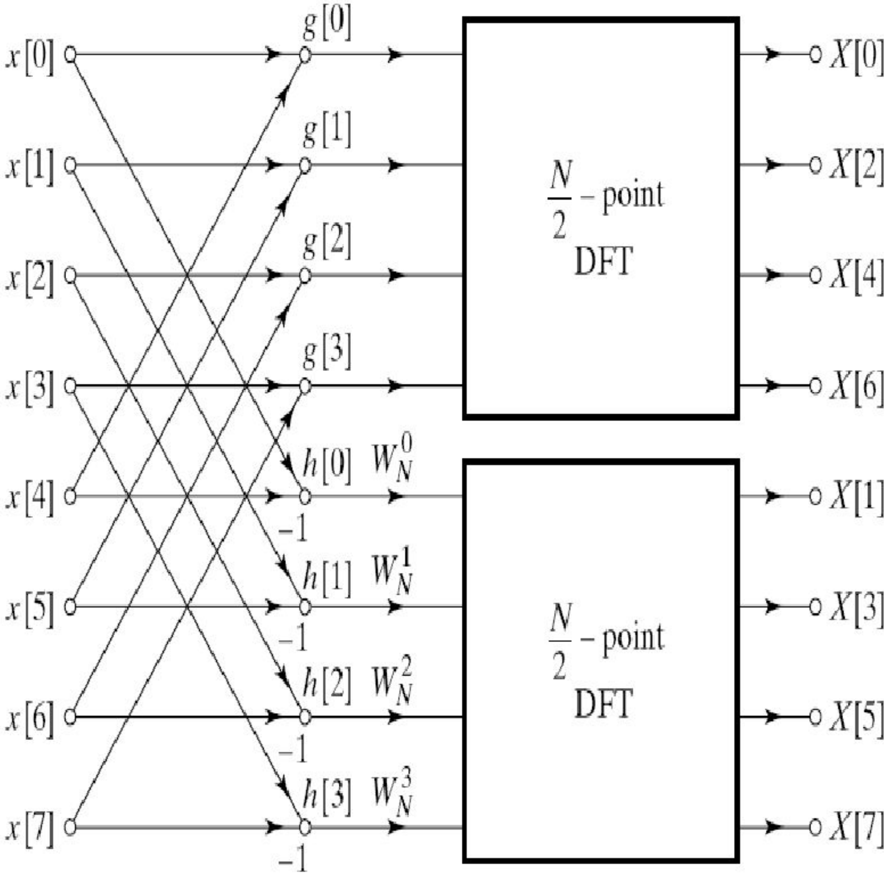


**Figure 9.17** Flow graph of decimation-in-frequency decomposition of an $N$-point DFT computation into two ($N/2$)-point DFT computations ($N = 8$).

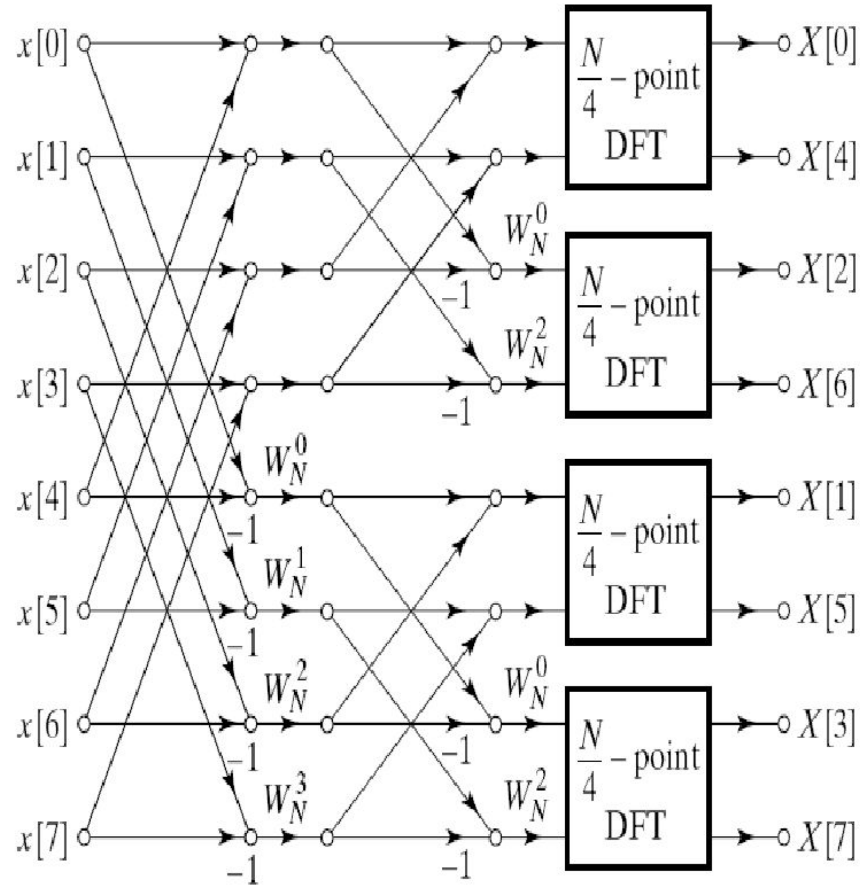


**Figure 9.18** Flow graph of decimation-in-frequency decomposition of an 8-point DFT into four 2-point DFT computations.

# Алгоритм Герцеля

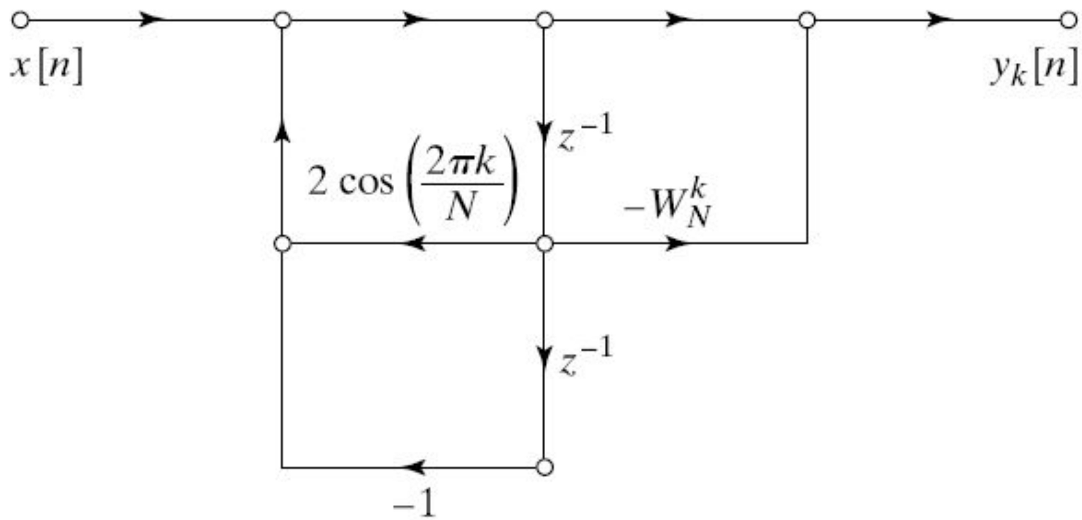


**Figure 9.2** Flow graph of second-order recursive computation of $X[k]$ (Goertzel algorithm).

**TABLE 5.2. Summary of Radial Fourier Transform Properties**

| Signal Expression | Radial Fourier Transform or Property |
|---|---|
| $f(t)$ | $F(\omega) = \int_{-\infty}^{\infty} f(t)e^{-j\omega t}dt$ (Analysis equation) |
| $f(t) = \frac{1}{2\pi}\int_{-\infty}^{\infty} F(\omega)e^{j\omega t}d\omega$ | $F(\omega)$ (Inverse, synthesis equation) |
| $af(t) + bg(t)$ | $aF(\omega) + bG(\omega)$ (Linearity) |
| $f(t-a)$ | $e^{-j\omega a}F(\omega)$ (Time shift) |
| $f(t)\exp(j\theta t)$ | $F(\omega - \theta)$ (Frequency shift, modulation) |
| $f(at)$, $a \neq 0$ | $\frac{1}{\|a\|}F\left(\frac{\omega}{a}\right)$ (Scaling, dilation) |
| $f(-t)$ | $F(-\omega)$ (Time reversal) |
| $\left\| \frac{d^n f(t)}{dt^n} \right\|$ | $(j\omega)^n F(\omega)$ (Time differentiation) |
| $(-jt)^n f(t)$ | $\frac{d^n}{d\omega^n}F(\omega)$ (Frequency differentiation) |
| $\\|x\\|_2 = \frac{\\|X(\omega)\\|_2}{\sqrt{2\pi}}$ | Plancherel's theorem |
| $\langle f, g\rangle = \frac{1}{2\pi}\langle F, G\rangle$ $f, g \in L^2(\mathbb{R})$ | Parseval's theorem |
| $f * h$, where $f, h \in L^2(\mathbb{R})$ | $F(\omega)H(\omega)$ |
| $f(t)h(t)$ | $(2\pi)^{-1}F(\omega) * H(\omega)$ |

| Periodic Sequence (Period $N$) | DFS Coefficients (Period $N$) |
|---|---|
| 1. $\tilde{x}[n]$ | $\tilde{X}[k]$ periodic with period $N$ |
| 2. $\tilde{x}_1[n], \tilde{x}_2[n]$ | $\tilde{X}_1[k], \tilde{X}_2[k]$ periodic with period $N$ |
| 3. $a\tilde{x}_1[n] + b\tilde{x}_2[n]$ | $a\tilde{X}_1[k] + b\tilde{X}_2[k]$ |
| 4. $\tilde{X}[n]$ | $N\tilde{x}[-k]$ |
| 5. $\tilde{x}[n-m]$ | $W_N^{km}\tilde{X}[k]$ |
| 6. $W_N^{-\ell n}\tilde{x}[n]$ | $\tilde{X}[k-\ell]$ |
| 7. $\sum_{m=0}^{N-1}\tilde{x}_1[m]\tilde{x}_2[n-m]$ (periodic convolution) | $\tilde{X}_1[k]\tilde{X}_2[k]$ |
| 8. $\tilde{x}_1[n]\tilde{x}_2[n]$ | $\frac{1}{N}\sum_{\ell=0}^{N-1}\tilde{X}_1[\ell]\tilde{X}_2[k-\ell]$ (periodic convolution) |
| 9. $\tilde{x}^*[n]$ | $\tilde{X}^*[-k]$ |

(*continued*)

| | | |
|---|---|---|
| 10. | $\tilde{x}^*[-n]$ | $\tilde{X}^*[k]$ |
| 11. | $\mathcal{R}e\{\tilde{x}[n]\}$ | $\tilde{X}_e[k] = \frac{1}{2}(\tilde{X}[k] + \tilde{X}^*[-k])$ |
| 12. | $j\mathcal{I}m\{\tilde{x}[n]\}$ | $\tilde{X}_o[k] = \frac{1}{2}(\tilde{X}[k] - \tilde{X}^*[-k])$ |
| 13. | $\tilde{x}_e[n] = \frac{1}{2}(\tilde{x}[n] + \tilde{x}^*[-n])$ | $\mathcal{R}e\{\tilde{X}[k]\}$ |
| 14. | $\tilde{x}_o[n] = \frac{1}{2}(\tilde{x}[n] - \tilde{x}^*[-n])$ | $j\mathcal{I}m\{\tilde{X}[k]\}$ |

Properties 15–17 apply only when $x[n]$ is real.

| | | |
|---|---|---|
| 15. | Symmetry properties for $\tilde{x}[n]$ real. | $\begin{cases} \tilde{X}[k] = \tilde{X}^*[-k] \\ \mathcal{R}e\{\tilde{X}[k]\} = \mathcal{R}e\{\tilde{X}[-k]\} \\ \mathcal{I}m\{\tilde{X}[k]\} = -\mathcal{I}m\{\tilde{X}[-k]\} \\ \lvert\tilde{X}[k]\rvert = \lvert\tilde{X}[-k]\rvert \\ \sphericalangle\tilde{X}[k] = -\sphericalangle\tilde{X}[-k] \end{cases}$ |
| 16. | $\tilde{x}_e[n] = \frac{1}{2}(\tilde{x}[n] + \tilde{x}[-n])$ | $\mathcal{R}e\{\tilde{X}[k]\}$ |
| 17. | $\tilde{x}_0[n] = \frac{1}{2}(\tilde{x}[n] - \tilde{x}[-n])$ | $j\mathcal{I}m\{\tilde{X}[k]\}$ |

| | Finite-Length Sequence (Length $N$) | $N$-point DFT (Length $N$) |
|---|---|---|
| 1. | $x[n]$ | $X[k]$ |
| 2. | $x_1[n], x_2[n]$ | $X_1[k], X_2[k]$ |
| 3. | $ax_1[n] + bx_2[n]$ | $aX_1[k] + bX_2[k]$ |
| 4. | $X[n]$ | $Nx[((-k))_N]$ |
| 5. | $x[((n-m))_N]$ | $W_N^{km}X[k]$ |
| 6. | $W_N^{-\ell n}x[n]$ | $X[((k-\ell))_N]$ |
| 7. | $\sum_{m=0}^{N-1} x_1(m)x_2[((n-m))_N]$ | $X_1[k]X_2[k]$ |
| 8. | $x_1[n]x_2[n]$ | $\frac{1}{N}\sum_{\ell=0}^{N-1} X_1(\ell)X_2[((k-\ell))_N]$ |
| 9. | $x^*[n]$ | $X^*[((-k))_N]$ |
| 10. | $x^*[((-n))_N]$ | $X^*[k]$ |
| 11. | $\mathcal{R}e\{x[n]\}$ | $X_{\text{ep}}[k] = \frac{1}{2}\{X[((k))_N] + X^*[((-k))_N]\}$ |
| 12. | $j\mathcal{I}m\{x[n]\}$ | $X_{\text{op}}[k] = \frac{1}{2}\{X[((k))_N] - X^*[((-k))_N]\}$ |
| 13. | $x_{\text{ep}}[n] = \frac{1}{2}\{x[n] + x^*[((-n))_N]\}$ | $\mathcal{R}e\{X[k]\}$ |
| 14. | $x_{\text{op}}[n] = \frac{1}{2}\{x[n] - x^*[((-n))_N]\}$ | $j\mathcal{I}m\{X[k]\}$ |
| Properties 15–17 apply only when $x[n]$ is real. | | |
| 15. | Symmetry properties | $\begin{cases} X[k] = X^*[((-k))_N] \\ \mathcal{R}e\{X[k]\} = \mathcal{R}e\{X[((-k))_N]\} \\ \mathcal{I}m\{X[k]\} = -\mathcal{I}m\{X[((-k))_N]\} \\ \lvert X[k]\rvert = \lvert X[((-k))_N]\rvert \\ \sphericalangle\{X[k]\} = -\sphericalangle\{X[((-k))_N]\} \end{cases}$ |
| 16. | $x_{\text{ep}}[n] = \frac{1}{2}\{x[n] + x[((-n))_N]\}$ | $\mathcal{R}e\{X[k]\}$ |
| 17. | $x_{\text{op}}[n] = \frac{1}{2}\{x[n] - x[((-n))_N]\}$ | $j\mathcal{I}m\{X[k]\}$ |

TABLE 10.2. Short-Time Fourier Transform Window Functions[a]

| Name | Definition |
|---|---|
| Rectangle | $w(t) = \begin{cases} b & \text{if } (\lvert t\rvert \le a) \\ 0 & \text{otherwise.} \end{cases}$ |
| Bartlett (triangle) | $w(t) = \begin{cases} \frac{b}{a}t + b & \text{if } -a \le t \le 0, \\ -\frac{b}{a}t + b & \text{if } 0 \le t \le a, \\ 0 & \text{otherwise.} \end{cases}$ |
| Hanning (von Hann) | $w(t) = \begin{cases} b\cos^2\left(\frac{\pi t}{2a}\right) & \text{if } \lvert t\rvert \le a \\ 0 & \text{otherwise.} \end{cases}$ |
| Hamming | $w(t) = \begin{cases} 0.54b + 0.46b\cos\left(\frac{\pi t}{a}\right) & \text{if } \lvert t\rvert \le a \\ 0 & \text{otherwise.} \end{cases}$ |
| Blackman | $w(t) = \begin{cases} 0.42b + 0.5b\cos\left(\frac{\pi t}{a}\right) + 0.08b\cos\left(\frac{2\pi t}{a}\right) & \text{if } \lvert t\rvert \le a \\ 0 & \text{otherwise.} \end{cases}$ |

[a]Adjust parameter $a > 0$ for a window width appropriate to the signal features of interest. Adjust parameter $b > 0$ in order to normalize the window function.

**TABLE 9.2. Window Functions for $N > 0$ Samples**[a]

| Name | Definition |
|---|---|
| Rectangular | $w(n) = \begin{cases} 1 & \text{if } \lvert n\rvert \le \dfrac{N-1}{2} \\ 0 & \text{otherwise} \end{cases}$ |
| Bartlett (triangular) | $w(n) = 1 - \dfrac{2\lvert n\rvert}{N-1} \quad \text{if } \lvert n\rvert \le \dfrac{N-1}{2}$ |
| Hann | $w(n) = \dfrac{1}{2}\left[1 - \cos\dfrac{2\pi n}{N-1}\right] \quad \text{if } \lvert n\rvert \le \dfrac{N-1}{2}$ |
| Hamming | $w(n) = 0.54 - 0.46\cos\dfrac{2\pi n}{N-1} \quad \text{if } \lvert n\rvert \le \dfrac{N-1}{2}$ |
| Blackman | $w(n) = 0.42 + 0.5\cos\dfrac{2\pi n}{N-1} + 0.08\cos\dfrac{4\pi n}{N-1} \quad \text{if } \lvert n\rvert \le \dfrac{N-1}{2}$ |
| Kaiser | $w(n) = \dfrac{I_0\left(\alpha\sqrt{1-\left(\dfrac{2n}{N-1}\right)^2}\right)}{I_0(\alpha)} \quad \text{if } \lvert n\rvert \le \dfrac{N-1}{2}$ |

# Форма и длинна временного окна

$$h[i] = K \frac{\sin(2\pi f_C (i - M/2))}{i - M/2} \left[ 0.42 - 0.5\cos\left(\frac{2\pi i}{M}\right) + 0.08\cos\left(\frac{4\pi i}{M}\right) \right]$$

EQUATION 16-3
Filter length vs. roll-off. The length of the filter kernel, $M$, determines the transition bandwidth of the filter, $BW$. This is only an approximation since roll-off depends on the particular window being used.

$$M \approx \frac{4}{BW}$$

**TABLE 3.1** SOME COMMON $z$-TRANSFORM PAIRS

| Sequence | Transform | ROC |
|---|---|---|
| 1. $\delta[n]$ | $1$ | All $z$ |
| 2. $u[n]$ | $\dfrac{1}{1-z^{-1}}$ | $\lvert z\rvert > 1$ |
| 3. $-u[-n-1]$ | $\dfrac{1}{1-z^{-1}}$ | $\lvert z\rvert < 1$ |
| 4. $\delta[n-m]$ | $z^{-m}$ | All $z$ except 0 (if $m > 0$) or $\infty$ (if $m < 0$) |
| 5. $a^n u[n]$ | $\dfrac{1}{1-az^{-1}}$ | $\lvert z\rvert > \lvert a\rvert$ |
| 6. $-a^n u[-n-1]$ | $\dfrac{1}{1-az^{-1}}$ | $\lvert z\rvert < \lvert a\rvert$ |
| 7. $na^n u[n]$ | $\dfrac{az^{-1}}{(1-az^{-1})^2}$ | $\lvert z\rvert > \lvert a\rvert$ |
| 8. $-na^n u[-n-1]$ | $\dfrac{az^{-1}}{(1-az^{-1})^2}$ | $\lvert z\rvert < \lvert a\rvert$ |
| 9. $[\cos\omega_0 n]u[n]$ | $\dfrac{1-[\cos\omega_0]z^{-1}}{1-[2\cos\omega_0]z^{-1}+z^{-2}}$ | $\lvert z\rvert > 1$ |
| 10. $[\sin\omega_0 n]u[n]$ | $\dfrac{[\sin\omega_0]z^{-1}}{1-[2\cos\omega_0]z^{-1}+z^{-2}}$ | $\lvert z\rvert > 1$ |
| 11. $[r^n\cos\omega_0 n]u[n]$ | $\dfrac{1-[r\cos\omega_0]z^{-1}}{1-[2r\cos\omega_0]z^{-1}+r^2z^{-2}}$ | $\lvert z\rvert > r$ |
| 12. $[r^n\sin\omega_0 n]u[n]$ | $\dfrac{[r\sin\omega_0]z^{-1}}{1-[2r\cos\omega_0]z^{-1}+r^2z^{-2}}$ | $\lvert z\rvert > r$ |
| 13. $\begin{cases} a^n, & 0 \le n \le N-1, \\ 0, & \text{otherwise} \end{cases}$ | $\dfrac{1-a^Nz^{-N}}{1-az^{-1}}$ | $\lvert z\rvert > 0$ |

**TABLE 8.1. Signals, Their $z$-Transforms, and the Region of Convergence of the $z$-Transform**

| $x(n)$ | $X(z)$ | $\mathrm{ROC}_X$ |
|---|---|---|
| $\delta(n-k)$ | $z^{-k}$ | $k>0: \{z \in \mathbb{C}^+: z \neq 0\}$ <br> $k<0: \{z \in \mathbb{C}^+ : z \neq \infty\}$ |
| $a^n u(n)$ | $z/(z-a)$ | $\{z \in \mathbb{C} : \|a\| < \|z\|\}$ |
| $-a^n u(-n-1)$ | $z/(z-a)$ | $\{z \in \mathbb{C} : \|z\| < \|a\|\}$ |
| $a^{-n} u(-n)$ | $\dfrac{1}{(1-az)}$ | $\{z \in \mathbb{C} : \|z\| < \|a\|^{-1}\}$ |
| $-a^{-n} u(n-1)$ | $\dfrac{1}{(1-az)}$ | $\{z \in \mathbb{C}^+ : \|z\| > \|a\|^{-1}\}$ |
| $na^n u(n)$ | $az/(z^2-2az+a^2)$ | $\{z \in \mathbb{C}^+ : \|a\| < \|z\|\}$ |
| $-na^n u(-n-1)$ | $az/(z^2-2az+a^2)$ | $\{z \in \mathbb{C} : \|z\| < \|a\|\}$ |
| $\cos(an)u(n)$ | $\dfrac{z^2-\cos(a)z}{z^2-2\cos(a)z+1}$ | $\{z \in \mathbb{C} : 1 < \|z\|\}$ |
| $\sin(an)u(n)$ | $\dfrac{\sin(a)z}{z^2-2\cos(a)z+1}$ | $\{z \in \mathbb{C} : 1 < \|z\|\}$ |
| $u(n)/(n!)$ | $\exp(z)$ | $\{z \in \mathbb{C}\}$ |
| $n^{-1}u(n-1)(-1)^{n+1}a^n$ | $\log(1+az^{-1})$ | $\{z \in \mathbb{C}^+ : \|a\| < \|z\|\}$ |

**TABLE 9.3. Summary of Laplace Transform Properties**

| Signal Expression | Laplace Transform or Property |
|---|---|
| $x(t)$ | $X_L(s) = \int_{-\infty}^{\infty} x(t)e^{-st}dt$ |
| $z(t) = ax(t) + by(t)$ | $aX_L(\omega) + bY_L(\omega)$<br>(Linearity, $\mathrm{ROC}_X \cap \mathrm{ROC}_Y \subseteq \mathrm{ROC}_Z$) |
| $y(t) = x(t-a)$ | $e^{-sa}X_L(s)$<br>(Time shift, $\mathrm{ROC}_X = \mathrm{ROC}_Y$) |
| $y(t) = x(t)\exp(at)$ | $X_L(s-a)$<br>(Frequency shift, modulation, $\mathrm{ROC}_Y = \{s: s-a \in \mathrm{ROC}_X\}$) |
| $y(t) = x(at),\ a \neq 0$ | $\frac{1}{\lvert a \rvert} XL_L\left(\frac{s}{a}\right)$<br>(Scaling, dilation, $\mathrm{ROC}_Y = \{s: s/a \in \mathrm{ROC}_X\}$) |
| $y(t) = (x * h)(t)$ | $F(s)H(s)$<br>(Convolution, $\mathrm{ROC}_X \cap \mathrm{ROC}_H \subseteq \mathrm{ROC}_Y$) |

# Преобразование Гильберта

$$H(k) = \begin{cases} 0 & \text{if } k = 0, \\ -j & \text{if } 1 \le k < \frac{N}{2}, \\ 0 & \text{if } k = \mathrm{N}/2, \\ j & \text{if } \frac{N}{2} < k \le N-1. \end{cases}$$

$$x_A(t) = x(t) + jx_H(t) .$$

$$x_A(t) = \left|x_A(t)\right| e^{j\phi(t)} ,$$

$$\phi(t) = \tan^{-1}\left[\frac{x_H(t)}{x(t)}\right] .$$

$$\left|x_A(t)\right| = \sqrt{x^2(t) + x_H^2(t)} .$$

$$\omega(t) = \frac{d}{dt}\phi(t) .$$

$$X(z) = \sum_{n=-\infty}^{+\infty} x(n) z^{-n}.$$

$$Y(z) = \sum_{n=-\infty}^{+\infty} y(n) z^{-n} = \sum_{n=-\infty}^{-1} -a^n z^{-n} = -\sum_{n=1}^{\infty} \left(\frac{z}{a}\right)^n = -\frac{z}{a} \sum_{n=0}^{\infty} \left(\frac{z}{a}\right)^n$$

$$= -\left(\frac{\frac{z}{a}}{1-\frac{z}{a}}\right) = \frac{z}{z-a},$$

$$X^+(z) = \sum_{n=0}^{+\infty} x(n) z^{-n},$$

$$X(z) = \sum_{n=-\infty}^{+\infty} x(n) z^{-n} = \sum_{n=0}^{\infty} a^n z^{-n} = \sum_{n=0}^{\infty} \left(\frac{a}{z}\right)^n = \frac{1}{1-\frac{a}{z}} = \frac{z}{z-a},$$

$$H(z) = \sum_{n=-\infty}^{+\infty} h(n) z^{-n} = \sum_{n=-2}^{+2} z^{-n} = z^{2n} + z^n + 1 + z^{-n} + z^{-2n}.$$

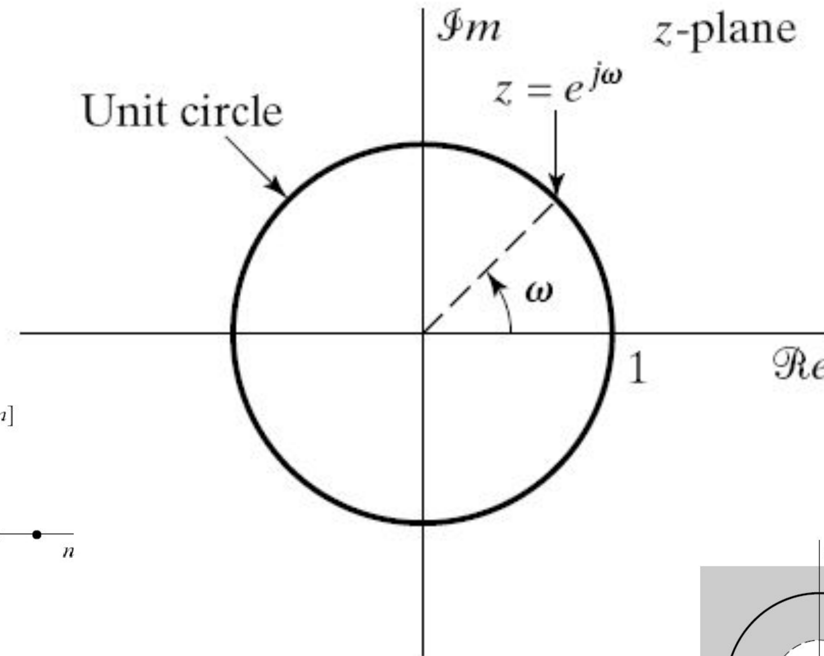


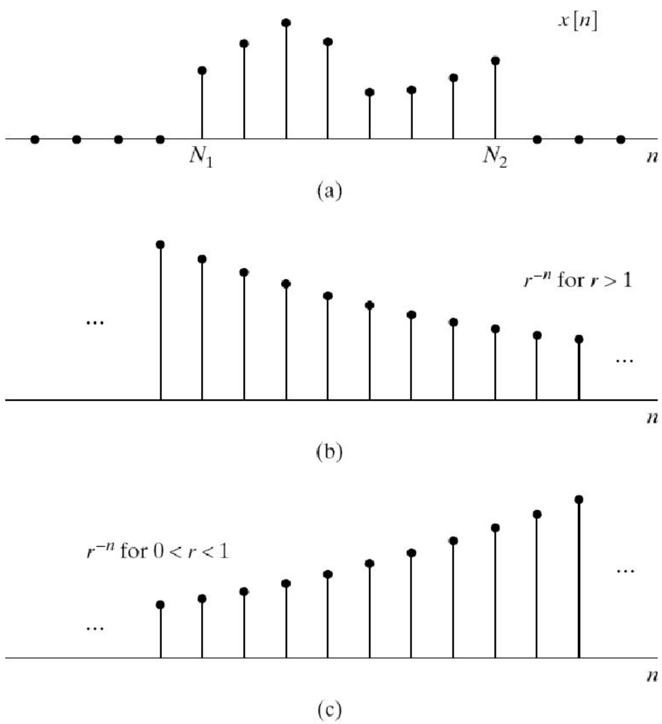


**Figure 3.8** Finite-length sequence and weighting sequences implicit in convergence of the $z$-transform. (a) The finite-length sequence $x[n]$. (b) Weighting sequence $r^{-n}$ for $1 < r$. (c) Weighting sequence $r^{-n}$ for $0 < r < 1$.

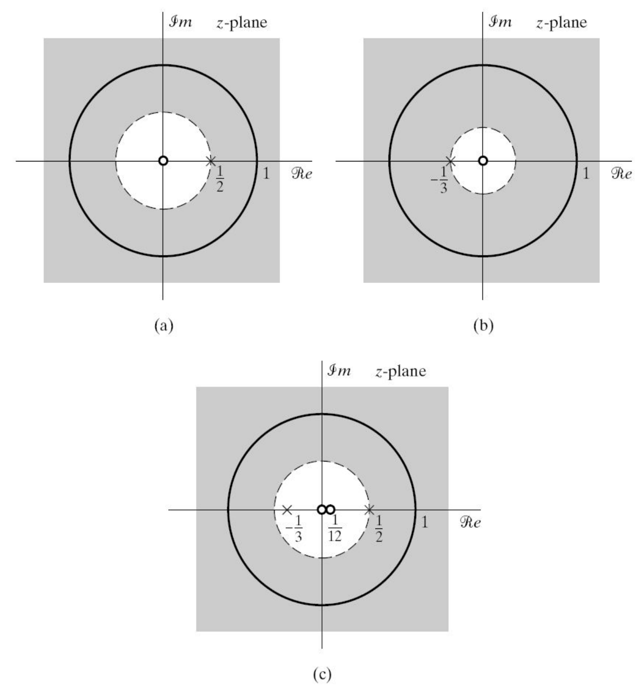


**Figure 3.5** Pole–zero plot and region of convergence for the individual terms and the sum of terms in Examples 3.3 and 3.4. (a) $1/(1 - \frac{1}{2}z^{-1})$, $|z| > \frac{1}{2}$. (b) $1/(1 + \frac{1}{3}z^{-1})$, $|z| > \frac{1}{3}$. (c) $1/(1 - \frac{1}{2}z^{-1}) + 1/(1 + \frac{1}{3}z^{-1})$, $|z| > \frac{1}{2}$.

**TABLE 9.7. Some Analog Hilbert Transform Properties**

| Signal Expression | Hilbert Transform or Property |
|---|---|
| $x(t)$ | $x_H(t) = \frac{1}{\pi} PV \int_{-\infty}^{\infty} \frac{x(s)}{t-s}\, ds = (\mathcal{H}x)(t)$ (Analysis equation) |
| $x_H(t)$ | $(\mathcal{H}x_H)(t) = -x$ (Inverse, synthesis equation) |
| $ax(t) + by(t)$ | $ax_H(t) + by_H(t)$ (Linearity) |
| $dx/dt$ | $dx_H/dt$ (Derivative) |
| $\langle x, x_H \rangle = \int_{-\infty}^{\infty} x(t)\overline{x_H(t)}\, dt = 0 \quad x \in L^2(\mathbb{R})$ | Orthogonality |
| $\lVert x \rVert_2 = \lVert x_H \rVert_2 \quad x \in L^2(\mathbb{R})$ | Energy conservation |

The inverse DTFT computation gives

$$h(n) = \frac{1}{2\pi}\int_{-\pi}^{\pi} H(\omega)e^{j\omega n}d\omega = \frac{j}{2\pi}\int_{-\pi}^{0} e^{j\omega n}d\omega + \frac{-j}{2\pi}\int_{0}^{\pi} e^{j\omega n}d\omega = \begin{cases} 0 & \text{if } n \text{ is even,} \\ \dfrac{2}{n\pi} & \text{if } n \text{ is odd.} \end{cases} \tag{9.176}$$

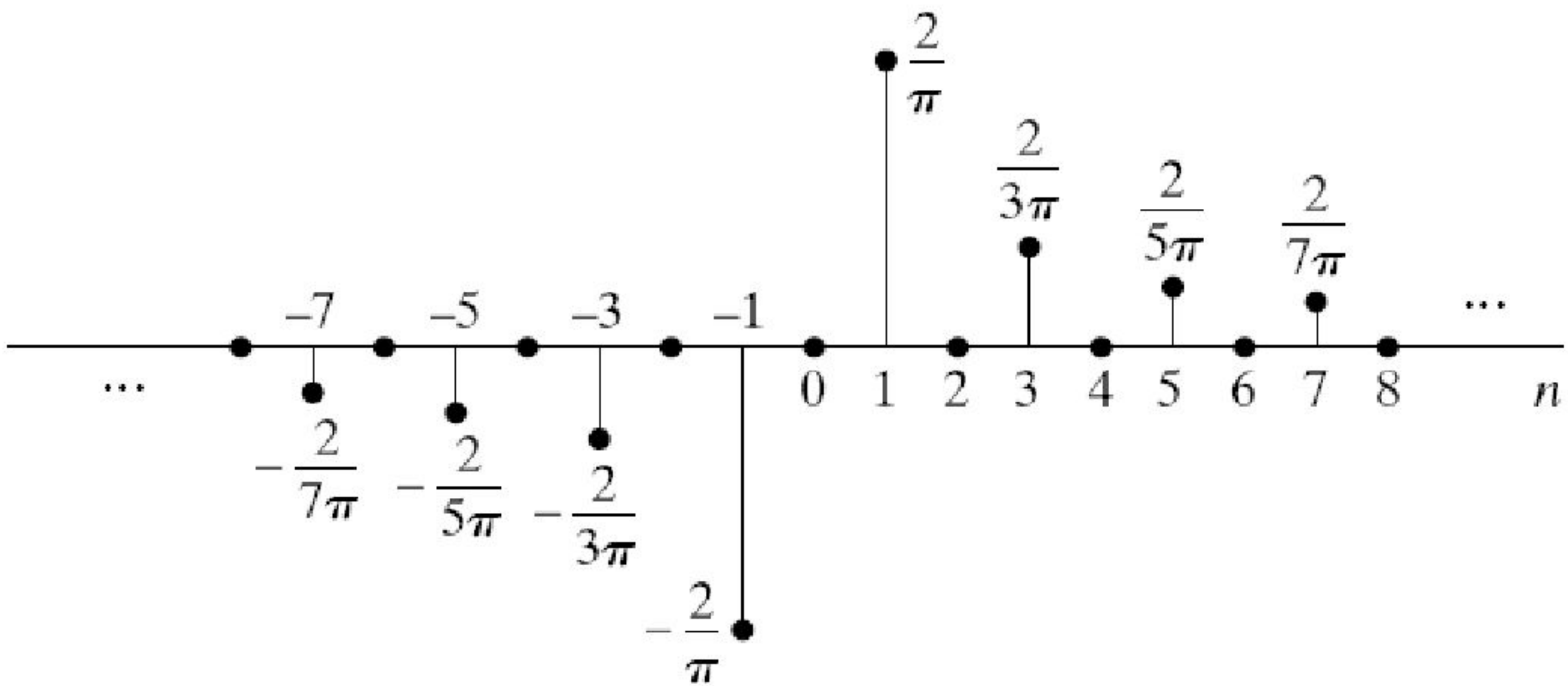


**Figure 11.5** Impulse response of an ideal Hilbert transformer or 90-degree phase shifter.

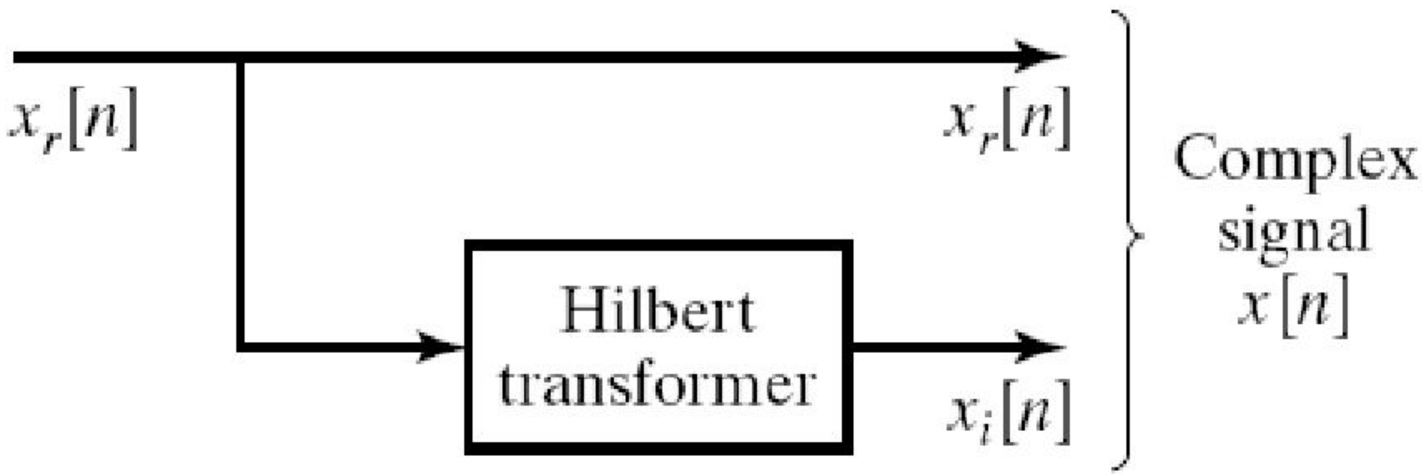


**Figure 11.6** Block diagram representation of the creation of a complex sequence whose Fourier transform is one sided.

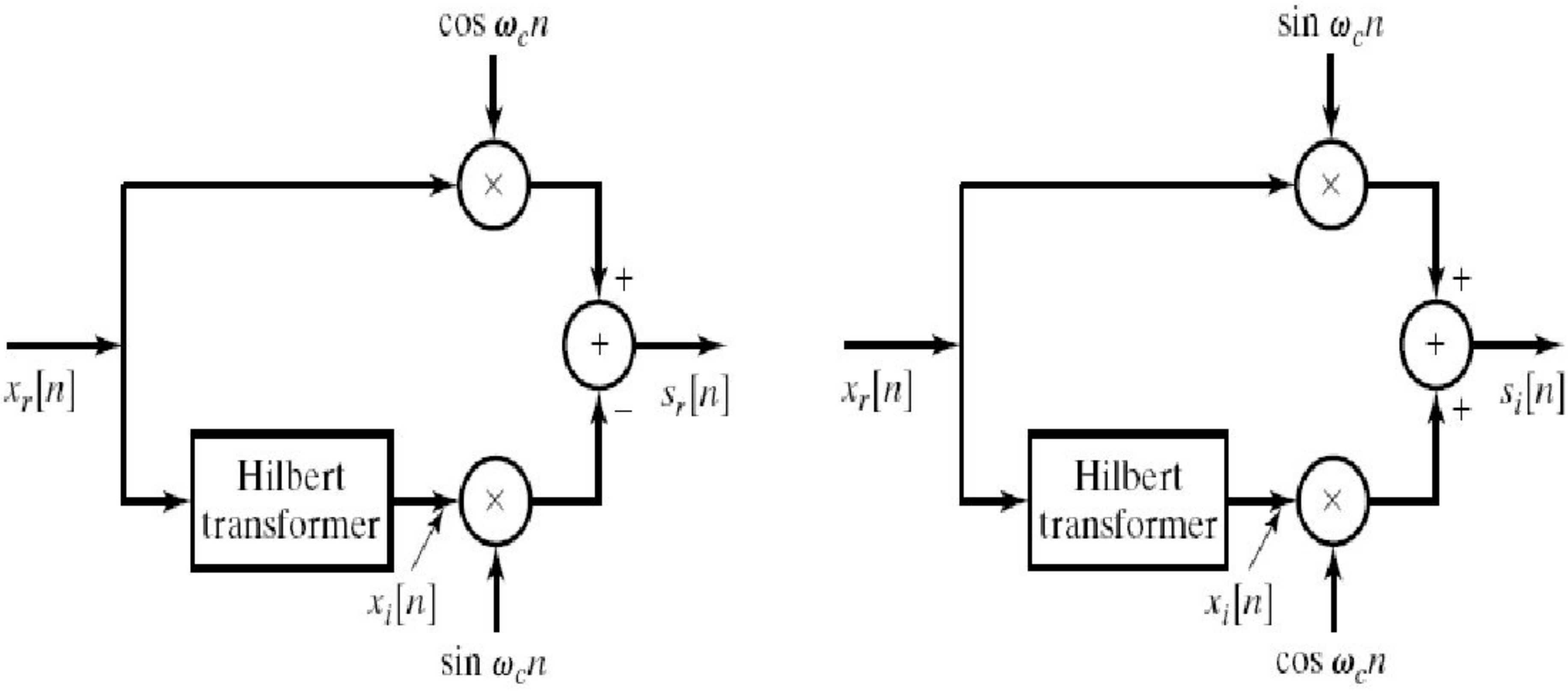


(a)

(b)

**Figure 11.11** Block diagram representation of Eqs. (11.76a) and (11.77a) for obtaining a single-sideband signal.

TABLE 11.1. Wavelet Transform Properties[a]

| Signal Expression | Wavelet Transform or Property |
|---|---|
| $\psi_{a,b}(t) = \frac{1}{\sqrt{\lvert a \rvert}}\psi\left(\frac{t-b}{a}\right)$ | Dilation and translation of $\psi(t)$ |
| $C_\psi = \int_{-\infty}^{\infty} \frac{\lvert \Psi(\omega) \rvert^2}{\lvert \omega \rvert}\, d\omega$ | Admissibility factor |
| $f(t)$ | $W[f(t)](a, b) = \int_{-\infty}^{\infty} f(t)\overline{\psi_{a,b}(t)}\, dt$ |
| $W[f(t)](a, b) = \frac{1}{\sqrt{2\pi}}\mathcal{F}[F(\gamma)](-b)$ | Fourier transform representation |
| $f(t) = \frac{1}{C_\psi}\int_{-\infty}^{\infty}\int_{-\infty}^{\infty} W[f(t)](a, b)\psi(t)\frac{da\,db}{a^2}$ | Inverse |
| $\theta(t) = \alpha\psi(t) + \beta\phi(t)$ | $W_\theta[f(t)] = \bar{\alpha}W_\psi[f(t)] + \bar{\beta}W_\phi[f(t)]$ |

[a]In the table, $\psi(t)$ is square-integrable.

**TABLE 10.1. Gabor Transform Properties**[a]

| Signal Expression | Gabor Transform or Property |
|---|---|
| $x(t)$ | $X_g(\mu, \omega)$ |
| $ax(t) + by(t)$ | $aX_g(\mu, \omega) + bY_g(\mu, \omega)$ |
| $x(t-a)$ | $e^{-j\omega a}X_g(\mu - a, \omega)$ |
| $x(t)\exp(j\theta t)$ | $X_g(\mu, \omega - \theta)$ |
| $\|x\|_2 = \sqrt{2\pi}\dfrac{\|X_g(\mu, \omega)\|_{2, L^2(R^2)}}{\|g\|_2}$ | Plancherel's theorem |
| $\langle x, y\rangle = \dfrac{1}{2\pi\|g\|_2^2}\langle X_g, Y_g\rangle$ | Parseval's theorem |
| $x(t) = \dfrac{1}{(2\pi\|g\|_2^2)}\int_{-\infty}^{\infty} X_g(\mu, \omega)g_{\mu, \sigma}(t)e^{j\omega t}d\omega d\mu$ | Inverse, resolution of the identity, or synthesis equation |

[a]In the table, $x(t)$ is square-integrable, and $g(t)$ is a Gaussian of mean $\mu$ and standard deviation $\sigma$.

**TABLE 10.3. Wigner–Ville Distribution Properties**[a]

| Signal Expression | WVD or Property |
|---|---|
| $x(t)$ | $X_{WV}(\mu, \omega)$ |
| $ax(t)$ | $\lvert a\rvert^2 X_{WV}(\mu, \omega)$ |
| $x(t) + y(t)$ | $X_{WV}(\mu, \omega) + Y_{WV}(\mu, \omega) + 2\mathrm{Real}[X_{WV,y}(\mu, \omega)]$ |
| $x(t - a)$ | $X_{WV}(\mu - a, \omega)$ |
| $x(t)\exp(j\theta t)$ | $X_{WV}(\mu, \omega - \theta)$ |
| $x(t)\exp(j\theta t^2)$ | $X_{WV}(\mu, \omega - 2\theta\mu)$ |
| $x(t/a)$, with a > 0 | $aX_{WV}(\mu/a, a\omega)$ |
| $X_{WV}(\mu, \omega) = \frac{1}{2\pi}\int_{-\infty}^{\infty} X\left(\omega + \frac{\theta}{2}\right)\overline{X\left(\omega - \frac{\theta}{2}\right)}e^{j\theta\mu}\,d\theta$ | Frequency-domain representation |
| $\int_{-\infty}^{\infty} X_{WV}(\mu, \omega)e^{-j\mu\theta}\,d\mu = X\left(\omega + \frac{\theta}{2}\right)\overline{X\left(\omega - \frac{\theta}{2}\right)}$ | Fourier transform of WVD |

[a]In this table, $x(t)$ and $y(t)$ are square-integrable.

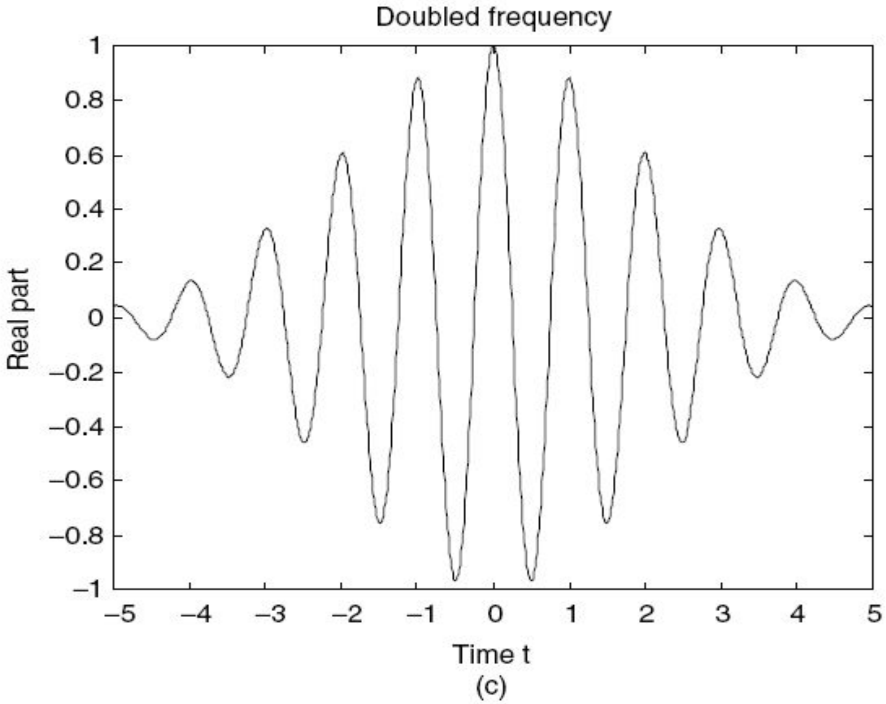


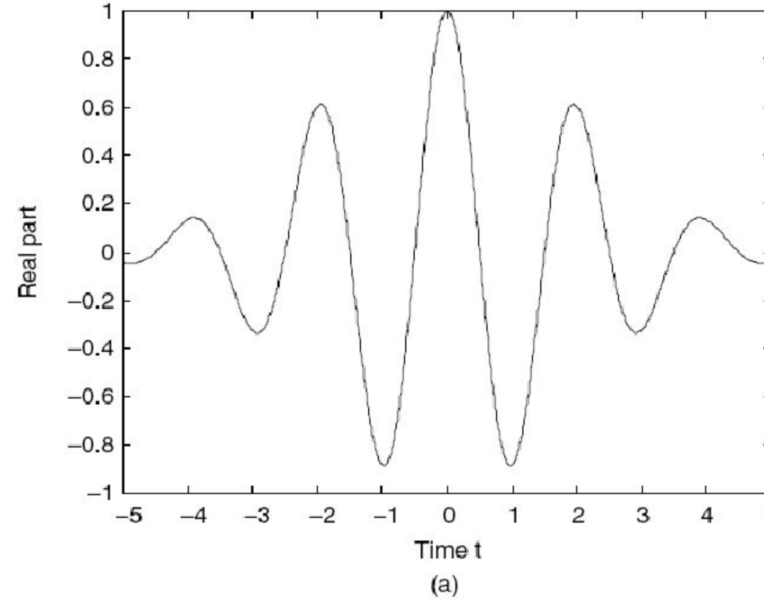


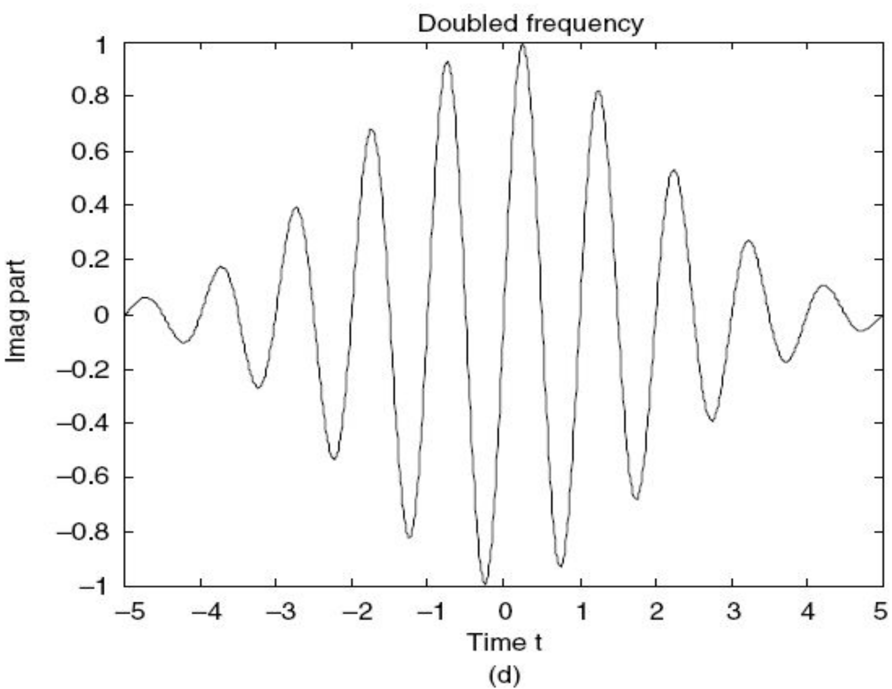


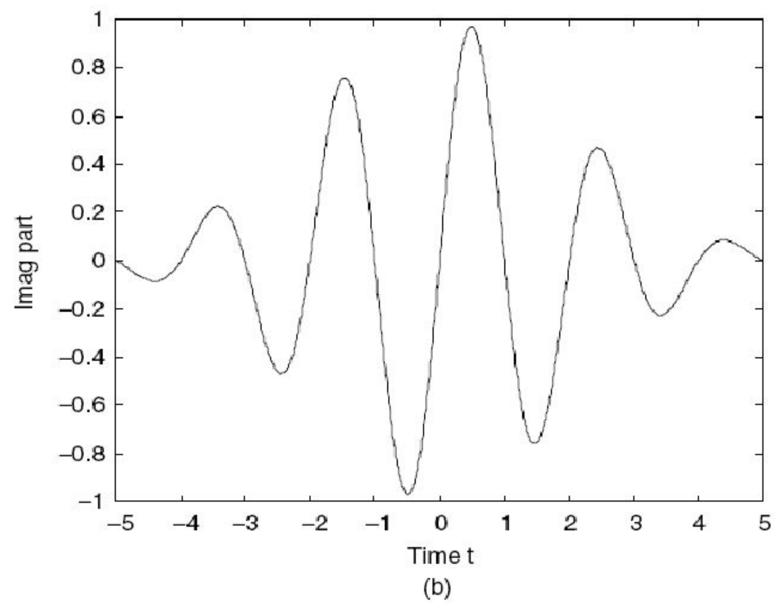


.2. Gabor elementary functions. The cosine term (a) represents the real part of a d is an even signal. The sine term represents the imaginary part and is an odd signal els (c) and (d) show the effect of frequency doubling.

# Свертка

$$\langle X,Y\rangle = \int_{-\pi}^{+\pi} X(\omega)\overline{Y}(\omega)\, d\omega = \int_{-\pi}^{+\pi}\left[\sum_{n=-\infty}^{+\infty} x(n)\exp(-j\omega n)\right]\left[\sum_{k=-\infty}^{+\infty} \overline{y}(k)\exp(j\omega k)\right]d\omega$$

$$= \int_{-\pi}^{+\pi}\left[\sum_{n=-\infty}^{+\infty}\sum_{k=-\infty}^{+\infty} x(n)\overline{y}(k)\exp^{-j\omega(n-k)}\right]d\omega. \qquad (7.60)$$

$$\langle X,Y\rangle = \sum_{n=-\infty}^{+\infty}\sum_{k=-\infty}^{+\infty}\int_{-\pi}^{+\pi} x(n)\overline{y}(k)\exp^{-j\omega(n-k)}\, d\omega = 2\pi\sum_{n=-\infty}^{+\infty} x(n)\overline{y}(n)$$

$$= 2\pi\langle x(n), y(n)\rangle.$$